学位論文

First-principles study of electron correlation in condensed matter with explicitly correlated wave functions

(露に相関した波動関数による
固体の電子相関効果の第一原理的研究)

平成 25 年 12 月　博士（理学）申請

東京大学大学院理学系研究科
物理学専攻

越智　正之

Abstract

First-principles electronic structure calculation is now regarded as an effective and powerful tool for studying condensed-matter physics. Most of the first-principles calculations for solids are carried out using the density functional theory (DFT), which provides the electronic structures with sufficient accuracy and low computational cost in many cases. Despite the great successes of DFT, generally-used approximations have serious drawbacks in accuracy, and to deal with this situation, the transcorrelated (TC) method, in which one uses the Jastrow-Slater-type many-body wave function, is one of the promising theories for accurate first-principles electronic structure calculations.

The TC method has several advantages for solid-state calculations; it partially takes account of some electron correlation effects such as the screening effect and short-range correlation by the Jastrow factor with reasonable computational cost, which is the same order of magnitude as the HF method, and the band structure and total energy can be obtained. Moreover, a similarity between the HF and TC methods allows ones to apply some sophisticated wave function theories, which conventionally use the one-electron orbitals and their orbital energies of the HF wave function, to the TC method just in the same way as the HF method. This possibility provides a simple way to improve accuracy of the TC method systematically. In spite of these great advantages, the TC method has a problem to overcome in accuracy, e.g., for the band gaps.

In this thesis, we achieved theoretical improvements for the TC method by two ways and apply them to the band structure calculations and excited state calculations of solids. The first way for improving accuracy is to optimize the Jastrow factor based on the random-phase approximation (RPA) and pseudo-variance minimization, and the other one is to apply the second-order Møller-Plesset (MP2) perturbation theory to the biorthogonal TC (BiTC) method. For both methods, we investigated their effects on the calculated band structures, and we found that (i) the long-range behavior of the Jastrow factor, which describes the screening effect of the electron-electron interaction, can be well optimized by our RPA treatment and the band gap of a large-gap insulator is improved, (ii) the short-range behavior of the Jastrow factor, however, does not affect the calculated band structures so much by using our Jastrow function with limited degrees of freedom, and

(iii) the BiTC-MP2 theory yields somewhat unsatisfactory results considering its expensive computational cost; the BiTC method, a starting point of the perturbation, shows good accuracy comparing with the HF method and then the calculated band gaps change very little by the MP2 correction in some cases. Theoretical investigation of the MP2 correction to the BiTC method suggests that the short-range correlation described with the Jastrow factor is important for calculating the accurate total energy, but the screening effect also plays an important role for the band structure calculations. These observations suggest that, to obtain more accurate band structures, we should describe the screening effect in more rigorous manner than the present treatment with only one Jastrow parameter.

Finally, we proposed a tractable method of excited state calculations by an extension of the TC method and applied it to calculations of the optical absorption spectra of solids using the optimized Jastrow function. Accurate excited-state calculations are also important for studying optical response or other rich phenomena related to the electron excitation. We verified that our method predicts the optical absorption spectra with satisfactory accuracy. Although this accuracy can be obtained also by other methods such as GW+BSE method, it is important that we can obtain the accurate optical absorption spectra and perform accurate excited state calculations using the TC method, which can provide both the total energy and accurate band structures.

Contents

1 Introduction **7**

1.1 Density functional theory (DFT) 7
1.2 Wave function theory 9
1.3 Transcorrelated (TC) method 10
1.4 Purpose of this study 12
1.5 Outline of this thesis 13

2 Transcorrelated (TC) method **17**

2.1 Basic idea 17
2.2 Derivation of the one-body self-consistent-field (SCF) equation 18
2.3 Jastrow factor 19

3 Optimization of the Jastrow factor **23**

3.1 Parameters in the Jastrow function 23
3.2 Optimization of the Jastrow factor: RPA 24
3.3 Optimization of the Jastrow factor: Pseudo-variance minimization 26
3.4 Calculation process 28
3.5 Conditions for our calculations 30
3.6 Results: RPA optimization 30
3.7 Results: pseudo-variance minimization 31

4 Biorthogonal formulation of the TC method (BiTC method) **39**

4.1 Formalism of the BiTC method 39
4.2 Differences between the TC and BiTC methods 40
4.3 Results: band gaps and total energies 41

5 The second-order Møller-Plesset (MP2) perturbation theory **43**

5.1 MP2 perturbation theory for the HF method 43
5.2 MP2 perturbation theory for the BiTC method 45
5.3 Band correction calculated by the MP2 perturbation theory 46

5.4 Computational cost 47
5.5 Results: convergence issues 47
5.6 Results: valence correlation energy 52
5.7 Results: band gaps 52
5.8 Role of the effective interaction in the TC Hamiltonian 53

6 Configuration Interaction Singles (CIS) method 57
6.1 HF-CIS method 57
6.2 TC-CIS method 58
6.3 Results: optical absorption spectra of solid LiF and GaAs 61

7 Conclusion 67

A Brillouin's theorem for the TC method 69

Chapter 1

Introduction

First-principles electronic structure calculation now plays an essential role in studying condensed-matter physics. Calculated electronic structures provide an important clue to understand the microscopic origins of various phenomena and properties observed in condensed matters. First-principles calculations also help one to interpret the experimental results such as spectra obtained by photoemission spectroscopy. Moreover, by these studies, one can obtain some guidelines for an efficient exploration of new devices for industrial applications. Despite these great significances, there are several problems to overcome in the study of the first-principles calculation. One of the most important issues is a problem of accuracy; it is still difficult to describe the electronic structures of some kinds of systems such as strongly correlated systems. We shall briefly review some kinds of methods for the first-principles electronic structure calculation especially from the viewpoint of accuracy. Hartree atomic units ($m_e = e^2 = \hbar = 1/(4\pi\epsilon_0) = 1$, where m_e, e, and ϵ_0 are the electron mass, elementary charge, and electric permittivity of free space, respectively.) are used throughout this thesis.

1.1 Density functional theory (DFT)

Density functional theory (DFT) [1, 2] is one of the most popular and successful approaches for first-principles electronic structure calculation of various systems including molecules and solids. We briefly describe its formalism and features in this section. We ignore a spin index of an electron in this section for simplicity.

The idea of the DFT is based on the two Hohenberg-Kohn theorems [1]. When we consider a many-particle system under an external potential $v(\mathbf{r})$, the theorems say that (i) $v(\mathbf{r})$ can be uniquely (to within an additive constant) determined by the realized ground-state particle density $n_0(\mathbf{r})$, and (ii) the ground-state total energy E is written as

$$E[n, v] = \int \mathrm{d}\mathbf{r} v(\mathbf{r}) n(\mathbf{r}) + F[n], \tag{1.1}$$

where $F[n]$ is a *universal functional*, that is, a functional independent on $v(\mathbf{r})$, and $n_0(\mathbf{r})$ gives minimum value of $E[n, v]$ for each $v(\mathbf{r})$. Then the many-body problem, which is usually described with a many-body function of $3N$-dimensional variables for N-particle systems, can be reduced to a variational problem of a 3-dimensional variable, $n(\mathbf{r})$. This simplification is a great advantage of the DFT, which enables us to tackle many-body problems with reasonable computational effort.

In addition, we always make use of the Kohn-Sham method [2]. This method is based on an assumption that the many-body problem of interacting particles under $v_{\text{ext}}(\mathbf{r})$ can be reduced to that of *non*-interacting particles under some external potential $v_{\text{eff}}(\mathbf{r})$, with the same ground-state particle density $n_0(\mathbf{r})$ and same total energy E as the original system being realized in the *non*-interacting system. In the Kohn-Sham method, one should solve a self-consistent-field (SCF) equation,

$$[-\frac{1}{2}\nabla^2 + v_{\text{eff}}(\mathbf{r})]\phi_i(\mathbf{r}) = \epsilon_i\phi_i(\mathbf{r}), \tag{1.2}$$

where ϕ_i is a one-electron orbital, ϵ_i is its orbital energy. $v_{\text{eff}}(\mathbf{r})$ is written as

$$v_{\text{eff}}(\mathbf{r}) = v_{\text{ext}}(\mathbf{r}) + \int \mathrm{d}\mathbf{r}' \frac{n(\mathbf{r}')}{|\mathbf{r} - \mathbf{r}'|} + \frac{\delta E_{xc}[n]}{\delta n}, \tag{1.3}$$

where the second term in the right-hand side is the Hartree potential and $E_{xc}[n]$ is called the *exchange-correlation energy functional*. Since $v_{\text{eff}}(\mathbf{r})$ depends on the particle density $n(r)$, Eq. (1.2) should be solved self-consistently. This SCF equation, called the Kohn-Sham equation, provides the band structure of solids, which is guaranteed by the Janak's theorem [3]. This is a great benefit of the DFT.

However, this strategy requires the exchange-correlation energy functional $E_{xc}[n]$, which includes all the difficulties of the many-body problem and so is quite non-trivial. The accuracy of DFT-based methods depends on the quality of the approximations for the exchange-correlation energy functional. Some simple approximations, such as the local density approximation (LDA) [4] and generalized gradient approximation (GGA) [5, 6], are widely used and provide satisfactory results in many cases. However, it is known that these approximations have serious drawbacks in accuracy, e.g., underestimation of the band gaps, inaccuracy of the activation energy in chemical reactions, and difficulty in describing strongly correlated systems or reproducing the London dispersion force. These shortcomings prevent broader applications of the first-principles calculations. While there are some developments in accuracy along the DFT formalism, such as hybrid DFT [7, 8, 9], DFT+U, and exchange-correlation functionals that can describe van der Waals interactions, it is still difficult to take account of various correlation effects all at once and find a systematic way for further improvement of accuracy.

1.2 Wave function theory

To resolve the difficulties in accuracy mentioned above, the wave function theory, another framework of the first-principles electronic structure calculation, is expected to be a promising alternative. In the wave function theory, one explicitly handles the many-body wave function of $3N$ dimension for the system of N interacting electrons, in contrast to the DFT where only 3-dimensional functions, one-electron orbitals and electron density, are used. Non-trivial Kohn-Sham mapping to the *non*-interacting systems used in the DFT formalism is not employed in the wave function theory. Because of these features, accuracy of the wave function theory can be improved by refining the $3N$-dimensional many-body wave function in a systematic manner.

The HF method, the simplest wave function theory, is a starting point of most of the other wave function theories. In the HF method, one assumes that the many-body wave function is represented with a single Slater determinant that consists of one-electron orbitals:

$$\Phi = \frac{1}{\sqrt{N!}}\det\begin{pmatrix} \phi_1(x_1) & \phi_1(x_2) & \cdots & \phi_1(x_N) \\ \phi_2(x_1) & \ddots & \ddots & \vdots \\ \vdots & \ddots & \ddots & \vdots \\ \phi_N(x_1) & \cdots & \cdots & \phi_N(x_N) \end{pmatrix}, \tag{1.4}$$

where ϕ_i is an one-electron orbital with the usual notation that x_i represents a position $\mathbf{r}_i$ and a spin σ_i of the i-th electron. To minimize the total energy of this trial wave function under the external potential $v_{\text{ext}}(x)$, one-electron orbitals should satisfy the following equation:

$$\left(-\frac{1}{2}\nabla_1^2 + v_{\text{ext}}(x_1)\right)\phi_i(x_1) + \sum_{j=1}^{N}\int \mathrm{d}x_2\ \phi_j^*(x_2)\frac{1}{|\mathbf{r}_1 - \mathbf{r}_2|}\det[\phi_{i,j}(x_{1,2})] = \epsilon_i\phi_i(x_1), \tag{1.5}$$

where $\det[\phi_{i,j}(x_{1,2})]$ means $\phi_i(x_1)\phi_j(x_2) - \phi_j(x_1)\phi_i(x_2)$ and one-electron orbitals are orthonormalized. We call this equation the HF-SCF equation, an operator which acts on $\phi_i(x_1)$ on the left-hand side of Eq. (1.5) the HF-Fock operator, and its matrix representation with some basis functions of one-electron orbitals the HF-Fock matrix hereafter. In other words, when we rewrite Eq. (1.5) as $\hat{h}(x_1)\phi_i(x_1) = \epsilon_i\phi_i(x_1)$, $\hat{h}(x_1)$ is the HF-Fock operator and $\langle\phi_{\text{basis},p}|\hat{h}|\phi_{\text{basis},q}\rangle$ is a (p,q) element of the HF-Fock matrix where ϕ_{basis} is a basis function used to expand the one-electron orbitals. This SCF equation is solved self-consistently, and the eigenvalues ϵ_i can be interpreted as the orbital energies. This is guaranteed by the Koopmans' theorem [10].

The HF method is very simple and known not to have enough accuracy for applications in many cases. In particular, for solid-state calculations, the HF method is known to largely overestimate the band gaps (e.g., about 7eV for bulk silicon while it experimentally has

the band gap of about 1 eV.) [11, 12, 13], because the HF method cannot describe the screening effect of the electron-electron Coulomb interaction. This fundamental effect is caused by a large number of interacting electrons and cannot be described with a mean-field approach like the HF method. It is also known that the density of states of the uniform electron gas unphysically vanishes at the Fermi energy in the HF method, owing to a logarithmic divergence of the derivative of the energy dispersion with respect to the wave vector. (see, e.g., Ref. [14].)

There are several wave function theories to improve accuracy beyond the HF method [15], for example, by considering linear combination of many Slater determinants constructed with the HF orbitals. This method is called the configuration interaction (CI) method. Other famous and successful examples are the Møller-Plesset (MP) perturbation theory, which is the many-body perturbation theory with the unperturbed Hamiltonian set to the HF-Fock operator, and the coupled-cluster (CC) theory. These methods that are based on and go beyond the HF wave function are called the post-HF methods.

Systematically improvable accuracy is an important advantage of these wave function theories, and is essential for high-accuracy calculation. However, the computational cost of these post-HF methods is often too expensive to apply to solid-state calculations. One of the reasons is a large number of electrons in solids, and another one is the need to consider many excited configurations owing to the inaccuracy of the HF method.

Therefore, it is desirable to discover another theory replacing the HF method as a starting point of the wave function theories for solid-state calculations. For this purpose, the transcorrelated (TC) method is one of the promising alternatives.

1.3 Transcorrelated (TC) method

The TC method [16, 17, 18, 19, 20, 21, 22, 23, 24, 25, 26, 27] is also one of the wave function theories. In this method, the many-body wave function is approximated as a product of a Jastrow factor, which is a symmetric product of a two-body positive function, and the Slater determinant. The many-body Hamiltonian is similarity-transformed by the Jastrow factor, and then the Shrödinger equation is transformed to an eigenvalue problem of the similarity-transformed Hamiltonian and its eigenstate is assumed to be the Slater determinant. In this sense, the TC method can be interpreted as the HF approximation applied to the similarity-transformed Hamiltonian. This similarity between the HF and TC methods is advantageous because the post-HF methods described in the previous section, such as the CI method and CC theory, can also be applied to the TC method, which enables one to improve accuracy of the TC method in a systematic manner. Moreover, electron correlation effects such as the screening effect are partially taken into account with the Jastrow factor in the TC method. In the TC calculation of the homogeneous electron

gas, it was reported that anomaly at the Fermi energy observed for the HF method does not appear [24, 28] and a fairly good estimate of the ground-state correlation energy was obtained [29]. Calculations of the total energies and band structures for some solids were performed and it was shown that the TC method is a great improvement over the HF method [24, 25] with the same order of magnitude of the computational cost as that of the HF method [25]. It is also remarkable that the Jastrow factor can describe the short-range correlation effects caused by such as the Coulomb hole and the electron-electron cusp condition [30], which cannot be described with the HF method and are considered to be the origins of slow convergence of CI expansions in highly accurate calculations of molecules. Therefore, the TC method can be a good replacement of the HF method for solid-state calculations.

Another aspect of the TC method is its relevance to the state-of-the-art quantum Monte Carlo (QMC) method [31], which also makes use of the Jastrow-Slater-type wave function. It is now established that QMC calculations provide very accurate total energy, and are widely applied to both molecules and condensed matters. In the QMC calculation, optimization of the one-electron orbitals in the Slater determinant is important in some cases [32] but difficult to achieve owing to its expensive computational cost. The TC method can be a fascinating way to optimize the one-electron orbitals with reasonable computational effort and has already been employed and combined with the fixed-node diffusion Monte Carlo (DMC) calculations for small atoms [33]. It is also noteworthy that the band structure, which can be easily obtained by the TC method, is computationally expensive to obtain by QMC calculations [34, 35].

Despite these great advantages, the TC method has some problems to overcome. One problem is that, though the TC method really improves the HF method, the calculated band gaps are not necessarily satisfactory in accuracy. Table 1.1, the data in which are taken from Table 3.2, presents the band gaps of some kinds of solids calculated using the LDA, HF, and TC methods. We can see that the TC method predicts the band gaps with good accuracy comparing with the LDA or HF method, but the band gaps of large-gap insulators, such as lithium chloride and lithium fluoride, are underestimated, and the band gap of silicon is a bit overestimated. Of course, when we consider the TC method as a starting point of systematic improvement of accuracy, these results are not discouraging, but at present, (i) there have been no studies that realizes systematic improvement of accuracy of the TC method for solid-state calculations, and moreover, (ii) the reason why the calculated band gaps exhibit the above-mentioned behavior is not clearly understood. Some post-HF methods combined with the TC method have been investigated and applied to molecular systems [21, 17, 36, 37, 38, 39], but not to solids yet.

	LDA	TC	HF	Exp.
Si	0.5[a]	1.7[a]	6.7[a]	1.17[b]
β-SiC	1.4[a]	2.4[a]	8.9[a]	2.4[c]
LiH	2.6	5.4	10.5	5.0[d]
C (diamond)	4.2[a]	5.9[a]	12.9[a]	5.48[c]
LiCl	6.2	8.6	15.5	9.4[e]
LiF	9.9	10.5	21.7	14.2[f]

Table 1.1: Band gaps (eV) for several solids calculated using various methods. These data are taken from Table 3.2. [a] Ref. [25], [b] Ref. [40], [c] Ref. [41], [d] Ref. [42], [e] Ref. [43], [f] Ref. [44].

1.4 Purpose of this study

In this study, we mainly concentrate on a problem: how one can predict the correct band structure by wave function theories. Correct band structures are indispensable, e.g., for treating the impurity problems, for which the relative position of the impurity level to the band structure of bulk solid is important, for studying the chemical reactions at the solid surfaces, and for predicting the optical response of solids. These issues are of much importance both for theoretical interests and for industrial applications, e.g., for electrochemical reactions or photocatalysis. Moreover, incorrect band gaps sometimes can falsely predict a metal to be an insulator, and vice versa. Though the well-known *GW* method [45, 46, 47], which is the many-body perturbation theory using the Green function, can predict the band structures of solids very accurately, it is still important to pursue the accurate band structure calculations by the wave function theory, because the *GW* method cannot be used for structural optimization. Hybrid DFT can provide relatively accurate band structures and also the total energies, but the self-interaction error, by which an electron is unphysically affected by the potential the electron itself produces, remains though the self-interaction error is suspected to be an origin of several inaccuracy of the DFT-based methods [48]. The TC method has no self-interaction error and can provide the total energy, and so development of the TC method is important for achieving accurate calculations and broadening the applicability of the first-principles calculation to condensed matter physics, but has not been investigated well for solid-state calculations.

For these purposes, in this thesis, we improve the Jastrow-Slater wave function used in the TC method by two ways. One way is to optimize the Jastrow factor, and the other one is to apply the second-order MP (MP2) perturbation theory to the similarity-transformed Hamiltonian, which means that "beyond a single Slater determinant" effects are partially included. For the former study, we develop a new method for optimization

aiming to determine the parameters in the Jastrow factor efficiently. Related to the latter study, we should note that the application of the post-HF methods such as the MP perturbation theory and CC theory to 3D solids have been actively reported in recent years [49, 50, 51, 52, 53], which shows that these post-HF methods are feasible in terms of the computational effort also for solid-state calculations. Of course, feasibility of the "post-TC" methods, i.e., the post-HF methods applied to the TC method, in terms of the computational cost should be carefully investigated because such a study has not been performed yet and the similarity-transformed Hamiltonian used in the TC method includes complicated interaction terms, which can increase the computational cost. We investigate how each approximation affects to the calculated band structures, and what kinds of correlation effects are retrieved in each theory. We often compare results obtained by the TC method with those for the HF method to clarify the role of the Jastrow factor. As a result of the improvements in accuracy, accurate excited-state calculations using the TC method are enabled. Accurate excited-state calculations are also important for studying optical response or other rich phenomena related to the electron excitation. Though some other methods such as the GW+BSE [54, 55, 56] method also can predict the accurate optical absorption spectra, it is important that we can obtain the accurate optical absorption spectra and perform accurate excited state calculations using the TC method, which can provide both the total energy and accurate band structures.

1.5 Outline of this thesis

A graphical abstract of this thesis is depicted in Figure 1.1. In Chapter 2, we will briefly review a formalism of the TC method. Our new method to optimize the Jastrow factor is presented in Chapter 3. Biorthogonal formalism of the TC method (BiTC method), which is required for applying the MP perturbation theory to the TC method, is described in Chapter 4. MP2 perturbation theory applied to the BiTC method is presented in Chapter 5. In Chapter 6, we perform the excited-state calculations using the improved Jastrow factor. Some results of test calculations are presented in each chapter. By these studies, we try to improve accuracy of the TC method, broaden its applicability to material science, and investigate how the electron correlation effects are retrieved (or not retrieved) by our explicitly correlated wave functions.

Another problem of the TC method not mentioned in previous sections is inaccuracy of the calculated lattice constants or bulk moduli, which are worse than those calculated using the LDA [25]. This issue seems to relate to the problem of the pseudopotential, i.e., treatment of the core electrons, because it is known that the choice of the pseudopotential can affect the accuracy of these quantities to some extent while the band structure are not affected so much. (see, e.g., [57].) This is an important future problem, but out of the

range of this thesis, and so not mentioned hereafter.

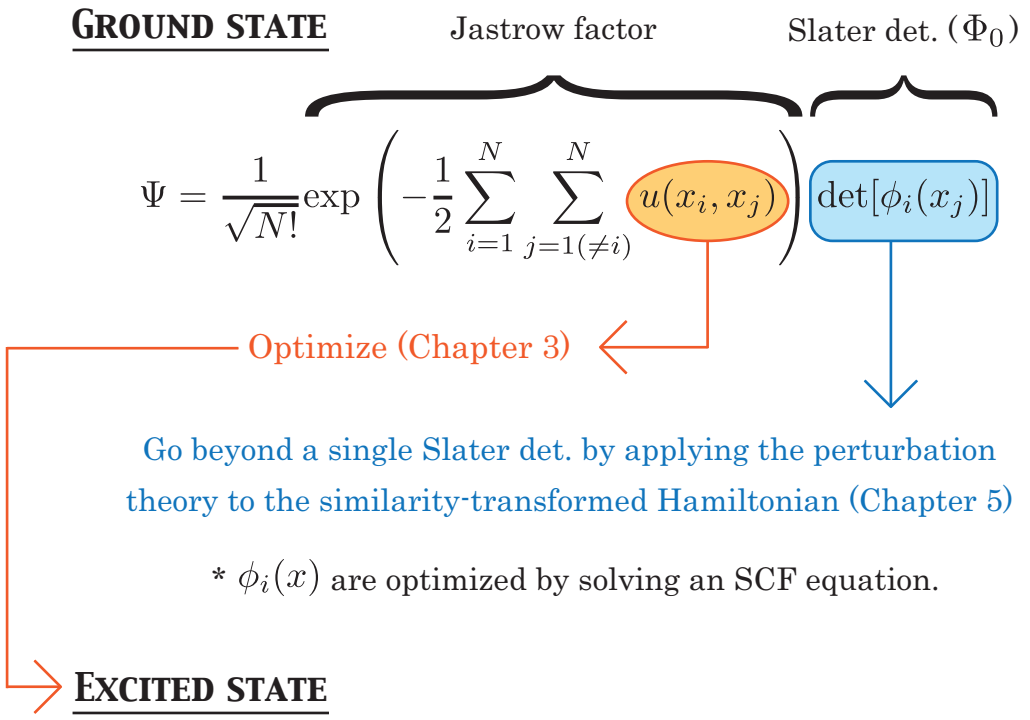

Figure 1.1: Graphical abstract of this thesis.

Chapter 2

Transcorrelated (TC) method

The TC method was proposed by Boys and Handy in late 1960's [16, 17, 18, 19, 20]. This method was recently reconstructed by Umezawa and Tsuneyuki [23], and description in this chapter is mainly based on it.

2.1 Basic idea

The basic idea of the TC method is taking into account the electron correlation effects through similarity transformation of the Hamiltonian. First, a many-body wave function Ψ is rewritten as $\Psi = F\Phi$: a product of the Jastrow factor F, which is a symmetric product of a two-body positive function,

$$F = \exp\left(-\frac{1}{2}\sum_{i=1}^{N}\sum_{j=1(\neq i)}^{N} u(x_i, x_j)\right) \tag{2.1}$$

where a Jastrow function $u(x_i, x_j)$ is symmetric with respect to an exchange of arguments, and a many-body function Φ formally defined as Ψ/F. Then the Schrödinger equation,

$$\mathcal{H}F\Phi = EF\Phi, \tag{2.2}$$

is completely equivalent to the similarity-transformed eigenvalue equation,

$$\begin{aligned} &\mathcal{H}_{TC}\Phi = E\Phi \\ &(\mathcal{H}_{TC} = F^{-1}\mathcal{H}F). \end{aligned} \tag{2.3}$$

When we apply the TC method to an electron system described with the Hamiltonian,

$$\mathcal{H} = \sum_{i=1}^{N}\left(-\frac{1}{2}\nabla_i^2 + v_{\mathrm{ext}}(x_i)\right) + \frac{1}{2}\sum_{i=1}^{N}\sum_{j=1(\neq i)}^{N}\frac{1}{|\mathbf{r}_i - \mathbf{r}_j|}, \tag{2.4}$$

the TC Hamiltonian $\mathcal{H}_{TC}$ is written as

$$\mathcal{H}_{TC} = \mathcal{H} + \frac{1}{2}\sum_{i=1}^{N}\sum_{j=1(\neq i)}^{N}(\nabla_i^2 u(x_i,x_j) - (\nabla_i u(x_i,x_j))^2 + 2\nabla_i u(x_i,x_j)\cdot\nabla_i) \\ -\frac{1}{2}\sum_{i=1}^{N}\sum_{j=1(\neq i)}^{N}\sum_{k=1(\neq i,j)}^{N}\nabla_i u(x_i,x_j)\cdot\nabla_i u(x_i,x_k). \tag{2.5}$$

In the TC method, Φ is assumed to be a single Slater determinant,

$$\Phi = \frac{1}{\sqrt{N!}}\det\begin{pmatrix}\phi_1(x_1) & \phi_1(x_2) & \cdots & \phi_1(x_N)\\ \phi_2(x_1) & \ddots & \ddots & \vdots\\ \vdots & \ddots & \ddots & \vdots\\ \phi_N(x_1) & \cdots & \cdots & \phi_N(x_N)\end{pmatrix}. \tag{2.6}$$

This can be interpreted as the HF approximation applied to the similarity-transformed Hamiltonian, and so the one-electron orbitals in the Slater determinant are optimized by solving an SCF equation like the HF method. This procedure is described in detail in the next section.

2.2 Derivation of the one-body self-consistent-field (SCF) equation

As for the HF method, the variational principle is employed to derive the one-body SCF equation. However, non-Hermiticity of the TC Hamiltonian owing to the non-unitarity of the Jastrow factor disables ones from applying the variational principle to the expectation value of the TC Hamiltonian,

$$E_{ps} = \frac{\langle\Phi|\mathcal{H}_{TC}|\Phi\rangle}{\langle\Phi|\Phi\rangle}. \tag{2.7}$$

Therefore the variance of the TC Hamiltonian for a real eigenvalue E is introduced:

$$\sigma_{TC}^2 = \frac{\langle\Phi|(\mathcal{H}_{TC}^\dagger - E)(\mathcal{H}_{TC} - E)|\Phi\rangle}{\langle\Phi|\Phi\rangle}, \tag{2.8}$$

and minimization of this quantity is employed as the guiding principle to optimize our trial wave functions. Now σ_{TC}^2 can be considered to be a function of $\{E, \Phi, \Phi^*, \mathcal{H}_{TC}\Phi, (\mathcal{H}_{TC}\Phi)^*\}$,

$$\sigma_{TC}^2 = \frac{\int(\mathcal{H}_{TC}\Phi)^*(\mathcal{H}_{TC}\Phi) - E\int((\mathcal{H}_{TC}\Phi)^*\Phi + \Phi^*(\mathcal{H}_{TC}\Phi)) + E^2\int\Phi^*\Phi}{\int\Phi^*\Phi}, \tag{2.9}$$

and a condition $\delta\sigma_{TC}^2/\delta\Phi^* = 0$ yields a one-body SCF equation for the TC method,[1]

$$\begin{aligned}
&\left(-\frac{1}{2}\nabla_1^2 + v_{\rm ext}(x_1)\right)\phi_i(x_1) \\
&+\sum_{j=1}^{N}\int {\rm d}x_2\ \phi_j^*(x_2)\Bigg(\frac{1}{|\mathbf{r}_1-\mathbf{r}_2|} + \frac{1}{2}\big(\nabla_1^2 u(x_1,x_2) + \nabla_2^2 u(x_1,x_2) \\
&-(\nabla_1 u(x_1,x_2))^2 - (\nabla_2 u(x_1,x_2))^2\big) + \nabla_1 u(x_1,x_2)\cdot\nabla_1 + \nabla_2 u(x_1,x_2)\cdot\nabla_2\Bigg) \\
&\times{\rm det}[\phi_{i,j}(x_{1,2})] - \frac{1}{2}\sum_{j=1}^{N}\sum_{k=1}^{N}\int {\rm d}x_2{\rm d}x_3\ \phi_j^*(x_2)\phi_k^*(x_3) \\
&\times\big(\nabla_1 u(x_1,x_2)\cdot\nabla_1 u(x_1,x_3) + \nabla_2 u(x_2,x_1)\cdot\nabla_2 u(x_2,x_3) + \nabla_3 u(x_3,x_1)\nabla_3 u(x_3,x_2)\big) \\
&\times{\rm det}[\phi_{i,j,k}(x_{1,2,3})] = \sum_{j=1}^{N}\epsilon_{ij}\phi_j(x_1),
\end{aligned} \tag{2.10}$$

where one-electron orbitals are orthonormalized. We call an operator which acts on $\phi_i(x_1)$ on the left-hand side of Eq. (2.10) the TC-Fock operator, and its matrix representation with some basis functions of one-electron orbitals the TC-Fock matrix, hereafter. The total energy E is evaluated as $E = {\rm Re}[E_{ps}]$, which is derived from a condition $\delta\sigma_{TC}^2/\delta E = 0$.[2]

It is noteworthy that we can avoid evaluation of $3N$-dimensional integrals usually required when we use the Jastrow-Slater-type wave function and calculate, for example, an expectation value of the total energy: $\langle\Phi F|\mathcal{H}|F\Phi\rangle/\langle\Phi F|F\Phi\rangle$. This is a great advantage of the TC method. Moreover, we can obtain the band structure because the Koopmans' theorem holds for ϕ_i and ${\rm Re}[\epsilon_{ii}]$ in the TC method alike for ϕ_i and ϵ_i in the HF method. Koopmans' theorem in the TC method states that the ionization energy (for the occupied states, the electron affinity for the unoccupied states) of ϕ_i equals to $-{\rm Re}[\epsilon_{ii}]$ if we take no account of orbital relaxation. This theorem provides physical meanings of one-electron orbitals and their energies.

2.3 Jastrow factor

While we can optimize the Slater determinant in the manner described in the previous section, to optimize the Jastrow factor is computationally much more expensive. One scheme uses the Fermi hypernetted-chain method [58, 59, 60, 61, 62], but it uses some approximations and is very complicated. The variational Monte Carlo (VMC) method,

[1] In more rigorous manner, σ_{TC}^2 should be treated as a function of $\{E, \phi_1, \phi_2, \ldots, \phi_N, \phi_1^*, \phi_2^*, \ldots, \phi_N^*, \mathcal{H}_{TC}\Phi, (\mathcal{H}_{TC}\Phi)^*\}$ and a condition $\delta\sigma_{TC}^2/\delta\phi_i^* = 0$ is used.

[2] How about other conditions? In fact, $\delta\sigma_{TC}^2/\delta\phi_i = 0$ yields Eq. (2.10), and both $\delta\sigma_{TC}^2/\delta(\mathcal{H}_{TC}\Phi) = 0$ and $\delta\sigma_{TC}^2/\delta(\mathcal{H}_{TC}\Phi)^* = 0$ yield Eq. (2.3).

which is a kind of the QMC methods, is nowadays the most popular approach to optimize the Jastrow factor using minimization of the total energy or its variance as the guiding principle. VMC has succeeded in predicting the electronic structure with high accuracy, but it is well known that QMC-based methods require high computational cost because they need to evaluate $3N$-dimensional integrations for the N-electron system. In addition, it is not easy to obtain the band structure using many k-points along the symmetry directions of solids using QMC methods, although the energy levels for some limited k-points are well reproduced by the fixed-node DMC calculations [35, 63, 64, 65, 66, 67, 68, 69].

Some alternative methods for the Jastrow-factor optimization based on the TC method have been proposed and applied to some atomic and molecular systems. Ten-no determines parameters in the Jastrow factor so that an effective two-body interaction of the TC Hamiltonian becomes small in the short-range region, and therefore these parameters are independent of the system under calculation [21]. This strategy works well for TC calculations as a starting point when combined with elaborate post-HF theories for molecular systems, but does not seem to work well for periodic systems because three-body terms of the TC Hamiltonian play an important role, i.e., describing the screening effect in periodic systems [70, 71, 28, 25], but are neglected in optimization process. An original set of equations for the TC method proposed by Boys and Handy includes an equation to optimize the Jastrow factor [17]. This equation was recently applied to some atomic and molecular systems by Luo *et al.* using Monte Carlo sampling [26]. Alternatively, Handy proposed minimization of the variance of the TC Hamiltonian and applied it to a helium atom [20] because the TC Hamiltonian is non-Hermitian and the variational principle does not hold, i.e., the minimization of the expectation value of the TC Hamiltonian does not work as the guiding principle for optimization. Later, Umezawa and Tsuneyuki developed the TC+VMC method, in which one uses Monte Carlo sampling to evaluate the variance of the TC Hamiltonian, and applied it to several small atomic systems [23]. However, these methods mentioned above are computationally expensive for solid-state calculations because many-body, such as five- or six-body, terms are involved. In regard to computational cost, a promising alternative was proposed and applied to a neon atom by Boys and Handy [17, 18]. There, some determinants like excited configurations were used to evaluate how far a trial wave function is from the exact eigenstate. They used a weighting factor for each configuration to achieve a practical computational cost at that time, but arbitrariness of the weighting factor seems to affect the results.

Owing to these difficulties, in previous works of the TC method for solids, we have used the following simple Jastrow function without adjustable parameters: [29, 24, 72, 25]

$$u(x, x') = \frac{A_0}{|\mathbf{r} - \mathbf{r}'|} \left(1 - \exp\left(-|\mathbf{r} - \mathbf{r}'|/C_{0;\sigma,\sigma'}\right)\right), \tag{2.11}$$

where $A_0 = \sqrt{V/(4\pi N)}$ (N: the number of valence electrons in the simulation cell, V: the volume of the simulation cell) and $C_{0;\sigma,\sigma'} = \sqrt{2A_0}$ (spin parallel: $\sigma = \sigma'$), $\sqrt{A_0}$ (spin anti-parallel: $\sigma \neq \sigma'$). The former condition is derived from the random-phase approximation (RPA) analysis of the uniform electron gas whose electron density is N/V [73], and the latter condition from the cusp condition [30]. Thus we can take the screening effect into account to some extent with the RPA and have the many-body wave function satisfy the cusp condition even though we use such a simple Jastrow function.

However, some unfavorable features exist in this function. First, we impose the conditions only for $|\mathbf{r}-\mathbf{r}'| \to \infty$ (RPA) and $|\mathbf{r}-\mathbf{r}'| \to 0$ (cusp condition), and so the intermediate region is not necessarily well described. Second, RPA is applied not to a target system but to the uniform electron gas, resulting in over-screening of the electron-electron Coulomb interaction, especially for wide-gap insulators. To resolve these problems, we develop a new scheme to optimize the Jastrow factor for periodic systems with reasonable computational effort, which is described in the next chapter.

Chapter 3

Optimization of the Jastrow factor

The Jastrow function used in the previous studies of the TC method for solid-state calculations, Eq. (2.11), has some unfavorable features described in the previous chapter. To resolve this problem, we develop a new scheme for optimizing the Jastrow factor for periodic systems. A part of contents in this chapter is published under licence in *J. Phys.: Conf. Ser.* by IOP Publishing Ltd. (M. Ochi and S. Tsuneyuki, *J. Phys.: Conf. Ser.* **454** 012020 (2013). http://iopscience.iop.org/1742-6596/454/1/012020).

3.1 Parameters in the Jastrow function

We use a more general form of the Jastrow function than the original form, Eq. (2.11). The Jastrow function used in this chapter is

$$\begin{aligned} u(x,x') = & \frac{A}{|\mathbf{r}-\mathbf{r}'|}\left(1-\exp\left(-|\mathbf{r}-\mathbf{r}'|/C_{\sigma,\sigma'}\right)\right) \\ & + \left(\sum_{m=0}^{M-1} c_{m;\sigma,\sigma'}\left(\frac{|\mathbf{r}-\mathbf{r}'|}{L}\right)^m\right) \\ & \times \left(\frac{|\mathbf{r}-\mathbf{r}'|}{L}-1\right)^3 \Theta\left(1-\frac{|\mathbf{r}-\mathbf{r}'|}{L}\right), \end{aligned} \tag{3.1}$$

where $\Theta(x)$ is the Heaviside step function defined as $\Theta(x) = 0\ (x<0),\ 1\ (x>0)$, and the cusp condition is always satisfied by imposing a constraint condition,

$$\frac{A}{2C_{\sigma,\sigma'}^2} + \frac{-3c_{0;\sigma,\sigma'} + c_{1;\sigma,\sigma'}}{L} = \frac{1}{4}\ (\sigma=\sigma'), \frac{1}{2}\ (\sigma\neq\sigma'), \tag{3.2}$$

throughout optimization of the Jastrow parameters. In this thesis, we call the first term of Eq. (3.1), $(A/|\mathbf{r}-\mathbf{r}'|)(1-\exp(-|\mathbf{r}-\mathbf{r}'|/C_{\sigma,\sigma'}))$, the long-range term because it describes asymptotic behavior at infinity ($|\mathbf{r}-\mathbf{r}'|\to\infty$); the remaining terms we call the short-range polynomials as these involve a cutoff length, L. No cutoff length is required for

the long-range term in the TC method because a special treatment exists for the $1/r$-type long-range function that was originally developed for the HF method by Gygi and Baldereschi [74]. The short-range polynomials have the same form as the Jastrow function used in Ref. [75], which is often used in QMC calculations of solids.

From the next section, we present our new method to optimize the parameters in the Jastrow function, Eq. (3.1). Our optimization process comprises two steps. First, the parameters in the long-range term in the Jastrow function are determined by using the RPA, described in Section 3.2. Next, the parameters in the short-range polynomials are optimized by the pseudo-variance minimization, described in Section 3.3.

3.2 Optimization of the Jastrow factor: RPA

First, the parameters in the long-range term of the Jastrow function (Eq. (3.1)), A and $C_{\sigma,\sigma'}$, are determined by using the dielectric constant ε calculated with the RPA relation. Using the RPA for this purpose is a natural idea because a long-range asymptotic form of the original Jastrow function, Eq. (2.11), was derived from the RPA analysis of the uniform electron gas [73]. We assume that the dielectric constant is isotropic; an anisotropic case, which is difficult to describe with only one long-range parameter A, is not investigated in this study.

When the Jastrow function has a long-range asymptotic form

$$u(x, x') \sim \frac{A}{|\mathbf{r}_1 - \mathbf{r}_2|} \quad (|\mathbf{r}_1 - \mathbf{r}_2| \to \infty), \tag{3.3}$$

the electron-electron Coulomb interaction in the TC-SCF equation, Eq. (2.10), is effectively screened as

$$\frac{1}{|\mathbf{r}_1 - \mathbf{r}_2|} \to \left(1 - (\frac{A}{A_0})^2\right) \frac{1}{|\mathbf{r}_1 - \mathbf{r}_2|} \quad (|\mathbf{r}_1 - \mathbf{r}_2| \to \infty). \tag{3.4}$$

This is caused by contributions from some three-body terms,

$$\begin{aligned} -\sum_{j=1}^{N}\sum_{k=1}^{N} \int \mathrm{d}x_2 \mathrm{d}x_3 \; & \phi_k^*(x_2)\phi_j^*(x_3) \\ & \times \nabla_3 u(x_3, x_1) \cdot \nabla_3 u(x_3, x_2) \det[\phi_{i,k}(x_{1,2})]\phi_j(x_3), \end{aligned} \tag{3.5}$$

which can be interpreted as the direct and exchange terms of the following two-body potential acting on ϕ_i,

$$\begin{aligned} & V_{\text{screen}}(x_1, x_2) \\ & \equiv \sum_{j=1}^{N} \int \mathrm{d}x_3 \; |\phi_j(x_3)|^2 \nabla_3 u(x_3, x_1) \cdot \nabla_3 u(x_3, x_2) \\ & = \int \mathrm{d}x_3 \; n(x_3) \nabla_3 u(x_3, x_1) \cdot \nabla_3 u(x_3, x_2), \end{aligned} \tag{3.6}$$

where $n(x)$ is the valence-electron density for the TC method. Eq. (3.5) can now be written as $-\sum_{k=1}^{N}\int \mathrm{d}x_2\phi_k^*(x_2)V_{\mathrm{screen}}(x_1,x_2)\det[\phi_{i,k}(x_{1,2})]$; cf. the direct and exchange term of the electron-electron Coulomb interaction acting on ϕ_i is $\sum_{k=1}^{N}\int \mathrm{d}x_2\phi_k^*(x_2)(1/|\mathbf{r}_1-\mathbf{r}_2|)\det[\phi_{i,k}(x_{1,2})]$. For the uniform electron gas, Eq. (3.4) is easily verified by substituting a plane wave for the one-electron orbital in the above equations: $\phi_l(\mathbf{r}) = (1/\sqrt{V})e^{i\mathbf{k}_l\cdot\mathbf{r}}$. We do not present the derivation here because it is a special case of a case mentioned below; moreover, a similar analysis of the uniform electron gas can be found in several articles [70, 71, 28, 25]. For general periodic systems, $V_{\mathrm{screen}}(x_1,x_2)$ depends not only on $\mathbf{r}_{12}=\mathbf{r}_1-\mathbf{r}_2$ but on $\mathbf{r}_M=(\mathbf{r}_1+\mathbf{r}_2)/2$ because of the inhomogeneity of the systems, therefore it should be averaged in terms of $\mathbf{r}_M$ to verify Eq. (3.4). Here we evaluate V_{screen} averaged over $\mathbf{r}_M$, using the Fourier transform by applying $(1/V)\int \mathrm{d}\mathbf{r}_{12}\exp(-i\mathbf{G}\cdot\mathbf{r}_{12})$ as follows:

$$
\begin{aligned}
&\left(\frac{1}{V}\int \mathrm{d}\mathbf{r}_{12}e^{-i\mathbf{G}\cdot\mathbf{r}_{12}}\right)\times\left(\frac{1}{V}\int \mathrm{d}\mathbf{r}_M\right)\times V_{\mathrm{screen}}(\mathbf{r}_1,\mathbf{r}_2)\\
&=\frac{1}{V^2}\int \mathrm{d}\mathbf{r}'\mathrm{d}\mathbf{r}''\mathrm{d}\mathbf{r}_3\ n(\mathbf{r}_3)\nabla u(\mathbf{r}')\cdot\nabla u(\mathbf{r}'')e^{-i\mathbf{G}\cdot(\mathbf{r}''-\mathbf{r}')}\\
&\qquad\qquad(\mathbf{r}'=\mathbf{r}_3-\mathbf{r}_1,\ \mathbf{r}''=\mathbf{r}_3-\mathbf{r}_2)\\
&=\frac{N}{V^2}\left|\int \mathrm{d}\mathbf{r}\ \nabla u(\mathbf{r})e^{-i\mathbf{G}\cdot\mathbf{r}}\right|^2\\
&\sim\frac{N}{V^2}\frac{(4\pi A)^2}{|\mathbf{G}|^2}\qquad(|\mathbf{G}|\to 0,\ \text{Eq. (3.3)})\\
&=\left(\frac{1}{V}\int \mathrm{d}\mathbf{r}_{12}e^{-i\mathbf{G}\cdot\mathbf{r}_{12}}\right)\times\left(\frac{A}{A_0}\right)^2\frac{1}{|\mathbf{r}_1-\mathbf{r}_2|},
\end{aligned}
\tag{3.7}
$$

where for simplicity the spin coordinates are omitted and the Jastrow function $u(\mathbf{r},\mathbf{r}')$ is assumed to be a function of $\mathbf{r}-\mathbf{r}'$. Therefore the electron-electron Coulomb interaction is partially canceled by the three-body terms, Eq. (3.5), and hence the screening occurs as Eq. (3.4).

For a more accurate treatment of the screening effect, we should not average the interaction over $\mathbf{r}_M$ and should use a more general form of the Jastrow function such as, e.g., $\sum_p w_p(\mathbf{r}_1)u_p(\mathbf{r}_1-\mathbf{r}_2)w_p(\mathbf{r}_2)$, which reflects the structure of materials and is frequently used in QMC calculations. Following this line of reasoning, Gaudoin *et al.* optimized the long-range behavior of the Jastrow function with the inhomogeneous RPA treatment, but reported that this method does not improve the accuracy as much when the cusp condition is imposed [76]. Therefore, at present, we adopt our simple approach to achieve a low-cost computation.

Using Eq. (3.4), we can determine the value of A as

$$
A = A_0\sqrt{1-\frac{1}{\varepsilon}}, \tag{3.8}
$$

where ε is the dielectric constant introduced to reproduce the electron-electron Coulomb interaction macroscopically screened as $1/(\varepsilon|\mathbf{r}-\mathbf{r}'|)$ for insulators. For metallic systems, we take $A = A_0$. Next, we determine the values of $C_{\sigma,\sigma'}$ to be

$$C_{\sigma,\sigma'} = \sqrt{2A}\ (\sigma = \sigma'),\ \sqrt{A}\ (\sigma \neq \sigma'), \tag{3.9}$$

to satisfy the cusp condition. To calculate ϵ for insulators, we use an RPA relation for LDA orbitals and band energies [77],

$$\varepsilon = 1 + \frac{8\pi}{V} \lim_{\mathbf{q}\to\mathbf{0}} \frac{1}{|\mathbf{q}|^2} \sum_{\mathbf{k},\sigma} \sum_{i}^{\text{occ.}} \sum_{a}^{\text{unocc.}} \frac{|\langle \phi^{\text{LDA}}_{\mathbf{k}+\mathbf{q},\sigma,a} | e^{i\mathbf{q}\cdot\mathbf{r}} | \phi^{\text{LDA}}_{\mathbf{k},\sigma,i} \rangle|^2}{\epsilon^{\text{LDA}}_{\mathbf{k}+\mathbf{q},\sigma,a} - \epsilon^{\text{LDA}}_{\mathbf{k},\sigma,i}}, \tag{3.10}$$

where i and a are indices of the occupied and unoccupied bands for the ground states, respectively, and $\mathbf{k}$ and $\mathbf{q}$ are wave vectors. Here we consider only electron-induced polarization because our purpose is to optimize the many-body wave function of electrons within the Born-Oppenheimer approximation. To evaluate the right-hand side of Eq. (3.10), we interpolate $\sum_{\mathbf{k},\sigma}\sum_i\sum_a |\langle \phi^{\text{LDA}}_{\mathbf{k}+\mathbf{q},\sigma,a}|e^{i\mathbf{q}\cdot\mathbf{r}}|\phi^{\text{LDA}}_{\mathbf{k},\sigma,i}\rangle|^2/(\epsilon^{\text{LDA}}_{\mathbf{k}+\mathbf{q},\sigma,a} - \epsilon^{\text{LDA}}_{\mathbf{k},\sigma,i})$ with a quadratic function of q_x, q_y, and q_z, and their coefficients determine the dielectric constant. Accuracy for the dielectric constant is much affected by the fineness of the k-point mesh in this procedure. Therefore, the resulting values of A corresponding to some finite numbers of k-points are extrapolated to that for an infinite number of k-points by fitting a quadratic function of the inverse of the number of k-points to the values of A. This is not an efficient way compared with that described in Ref. [77], but simple to implement and even if using this way, its computational cost is actually much smaller than the total cost. In addition, convergence of A in terms of the number of k-points is verified in our calculations.

3.3 Optimization of the Jastrow factor: Pseudo-variance minimization

Next, we determine the remaining parameters in the Jastrow function (Eq. (3.1)), $c_{m;\sigma,\sigma'}$ and L, including in the short-range polynomials. For this purpose, we rewrite the variance of $\mathcal{H}_{\text{TC}}$, called the TC variance, as follows:

$$\sigma^2_{\text{TC}} = \langle\Phi_0|(\mathcal{H}^\dagger_{\text{TC}} - E_0)(\mathcal{H}_{\text{TC}} - E_0)|\Phi_0\rangle \tag{3.11}$$

$$= \sum_p^\infty \langle\Phi_0|\mathcal{H}^\dagger_{\text{TC}} - E_0|\Phi_p\rangle\langle\Phi_p|\mathcal{H}_{\text{TC}} - E_0|\Phi_0\rangle \tag{3.12}$$

$$= \sum_p^\infty |\langle\Phi_p|\mathcal{H}_{\text{TC}} - E_0|\Phi_0\rangle|^2, \tag{3.13}$$

where Φ_p satisfies the completeness relation, $\sum_p^\infty |\Phi_p\rangle\langle\Phi_p| = \text{id}$. The TC variance exhibits some favorable features: (i) it is a non-negative real number, (ii) it equals zero if $\mathcal{H}_{\text{TC}}\Phi_0 =$

$E_0\Phi_0$ exactly holds, and (iii) if $\mathcal{H}_{\rm TC}\Phi_0 \neq E_0\Phi_0$ then the TC variance is larger than zero. In this sense, minimizing the TC variance is a good guiding principle to optimize the parameters in the Jastrow function, but it is computationally extremely demanding because the TC variance involves a six-body potential in $\mathcal{H}_{\rm TC}^\dagger\mathcal{H}_{\rm TC}$ and an infinite sum in terms of p in Eq. (3.13). Even if the summation over 'p' in Eq. (3.13) is limited to some finite number of 'p', (i) and (ii) still hold, but (iii) does not. However, this quantity still can be a good measure to gauge how Φ_0 is far from the exact eigenstate. Therefore, we define the pseudo-variance as

$$\sigma_{\rm PS}^2 = \sum_p^{\rm finite} |\langle\Phi_p|\mathcal{H}_{\rm TC} - E_0|\Phi_0\rangle|^2, \tag{3.14}$$

and employ its minimization as the guiding principle for optimizing the Jastrow function. This approach was originally proposed by Boys and Handy [17, 18], but they use a slightly different quantity,

$$\sum_p^{\rm finite} \frac{|\langle\tilde{\Phi}_p|\mathcal{H}_{\rm TC} - E_0|\Phi_0\rangle|^2}{\Delta E}$$
$$(\Delta E = \langle\tilde{\Phi}_p|\mathcal{H}_{\rm TC}|\tilde{\Phi}_p\rangle - \langle\Phi_0|\mathcal{H}_{\rm TC}|\Phi_0\rangle), \tag{3.15}$$

where $\tilde{\Phi}_p$ are determinants with one or two orbitals in the Slater determinant of the ground state being replaced with some basis functions, and $(\Delta E)^{-1}$ is called a weighting factor, which suppresses contribution from $\tilde{\Phi}_p$ of high energy. The weighting factor was necessary to perform calculations under practical computational cost for that time, but there is no specific reason to choose this form of the weighting factor. Different choices may produce different results. Moreover, minimization of this guiding variable can in principle yield unstable behavior, because it is not necessarily positive if we change the values of the Jastrow parameters for fixed Φ_0 and $\tilde{\Phi}_p$. To overcome these problems, we eliminated the weighting factor. Without the weighting factor, we can relate the pseudo-variance to the TC variance in the way described at the beginning of this section. It is interesting that variance minimization in the VMC calculation uses a similar idea to ours; that is, the variance for a small number of samplings can be a guiding variable for optimization [78].

In principle, the choice of Φ_p is arbitrary, and we choose doubly excited configurations, $\Phi_{i,j}^{a,b} \equiv (1/\sqrt{N!})\det[\phi_{1,2,\ldots,\hat{i},\ldots,\hat{j},\ldots,N-1,N,a,b}(x_{1,\ldots,N})]$, where electrons of the i-th and j-th occupied states of the ground state are excited to the a-th and b-th unoccupied states. Here, because of the Brillouin's theorem for the TC method, $\langle\Phi_p|\mathcal{H}_{\rm TC}|\Phi_0\rangle = 0$ for a singly excited configuration, proved in the Appendix. Additionally, contributions from a configuration involving excitations of more than three electrons equal zero because the similarity-transformed Hamiltonian consists of up to three-body interactions. The contribution from a triply excited configuration is non-zero but its calculation is computationally very expensive, hence not considered here. In addition, for an efficient calculation,

we restrict the electron excitations. We use N_k as the number of k-point in solving the TC-SCF equation Eq. (2.10) to obtain the one-electron orbitals and in describing the occupied orbitals in the determinants, but we also use $N_{k,mini}$ as the number of k-points where the electron excitation should be included with $N_{k,mini}$ taken to be smaller than N_k. In other words, for a doubly excited configuration $\Phi_{i,j}^{a,b}$, one-electron orbitals involved with electron excitations, ϕ_i, ϕ_j, ϕ_a, and ϕ_b, should be chosen from a small, $N_{k,mini}$, k-point mesh to lower computational cost, while occupied orbitals $\phi_{1,\ldots,N}$ belong to an N_k k-point mesh. This idea that one can use different values between N_k and $N_{k,mini}$ was used in MP2 calculations for one-dimensional periodic molecules by Shimazaki *et al.* [79].

Because $c_{m;\sigma,\sigma'}$ are linear parameters in the Jastrow function, the pseudo-variance is written as a polynomial of $c_{m;\sigma,\sigma'}$ (cf. Eq. (2.5), (3.1), and (3.14)). This fact enables us to optimize these parameters efficiently because once we calculate the coefficients of this polynomial at the beginning of the whole optimization process, the values of the pseudo-variance and its gradient for each optimization step are obtained at very low computational cost. A similar situation is investigated for some VMC calculations [80]. Similarly to the approach in this reference, we use the Broyden-Fletcher-Goldfarb-Shanno (BFGS) method [81, 82, 83, 84] for pseudo-variance minimization, which is well known to be a robust and efficient method for minimization problems. In contrast, the optimization of the value of L is computationally costly because it appears non-linearly in the Jastrow function. Therefore, we determine its value for now from $(4/3)\pi L^3 = V_{\text{unit cell}} N_{k,mini}$, where $V_{\text{unit cell}}$ is the volume of the unit cell. In this choice, we use the largest value of L within the size of the region, for which the periodic boundary condition is imposed for Φ_p. A similar choice for L is often taken in QMC calculations.

Pseudo-variance minimization requires computational cost of $\mathcal{O}(((N_k N_{k,mini}^2 N_{b,filled} N_{bv}^2) + (N_{k,mini}^3 N_{bv}^2 N_{bc}^2)) N_{pw})$, where $N_{b,filled}$ denotes the number of valence bands for the ground state, and the electron excitation for doubly excited configurations is restricted to an $N_{k,mini}$ k-point mesh, $N_{bv} (\leq N_{b,filled})$ valence bands, and N_{bc} conduction bands from the Fermi energy. N_{pw} is the number of plane waves used in expanding the one-electron orbitals. An overall computational cost strongly depends on how many excited configurations are required, and we will present some related results in a later section.

3.4 Calculation process

Overall calculation process is presented in Figure 3.1. First, we perform an LDA calculation. Next, the dielectric constant ε is calculated with the RPA relation, Eq. (3.10), using LDA orbitals. This is a similar procedure as the GW method [45, 46, 47], which is now well known to be a reliable first-principles method for solid-state calculations. Using the calculated dielectric constant, Eq. (3.8), and Eq. (3.9), we can determine the values of A

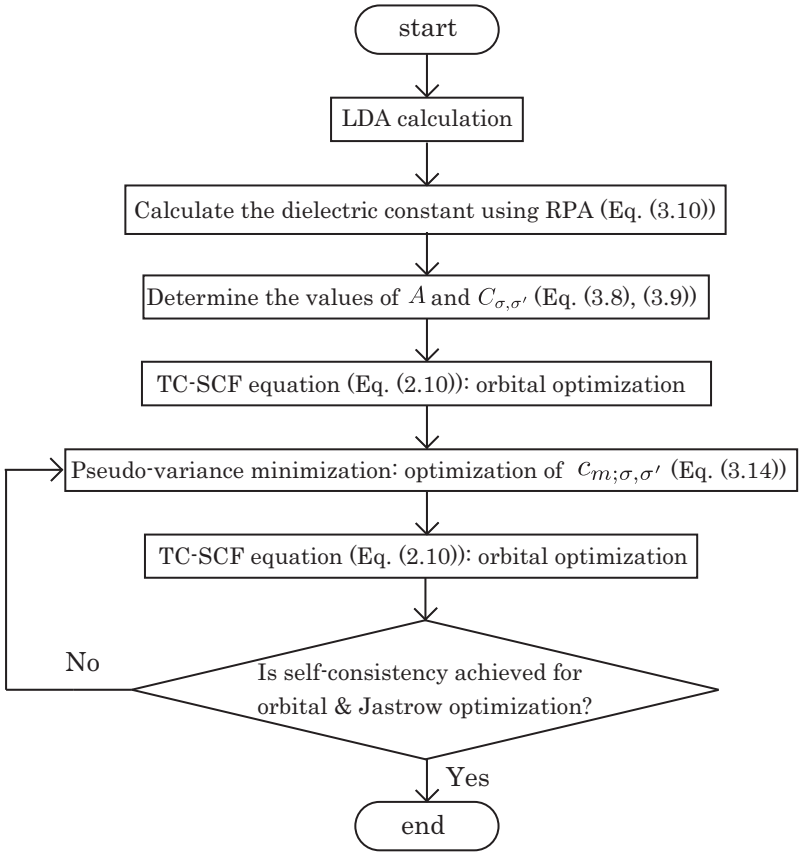

Figure 3.1: Calculation process for full optimization of the Jastrow-Slater-type wave function by the TC method.

and $C_{\sigma,\sigma'}$ in the Jastrow function. The TC-SCF equation, Eq. (2.10), is then solved with $u(x,x') = (A/|\mathbf{r}-\mathbf{r}'|)\left(1-\exp\left(-|\mathbf{r}-\mathbf{r}'|/C_{\sigma,\sigma'}\right)\right)$, to optimize the one-electron orbitals of the TC method for this initial Jastrow function. Now we use a Jastrow function with the short-range polynomials, Eq. (3.1), and optimize the coefficients $c_{m;\sigma,\sigma'}$ using the pseudo-variance minimization, Eq. (3.14). In this procedure, we use $c_{m;\sigma,\sigma'} = 0$ for the initial guess. For bulk silicon with $M = 4$, we also tried other initial guesses constructed with random values, but for most sets of initial values, we reached the same minimum for the pseudo-variance as that for $c_{m;\sigma,\sigma'} = 0$. In the other cases we reached only one other local minimum but its pseudo-variance value is several times as large as the lowest value. These results support our idea to use $c_{m;\sigma,\sigma'} = 0$ as an initial guess to reach the global minimum for bulk silicon. Finally, we obtain physical quantities such as the band gap and the total energy by solving the TC-SCF equation again. Optimization of the Jastrow factor and that for one-electron orbitals should be repeated self-consistently, but we verified that the results presented in this paper are almost unchanged by such self-consistent iterations.

3.5 Conditions for our calculations

One-electron orbitals in the HF and TC methods were expanded with LDA [4] orbitals in our study. These LDA basis functions were used only to reduce the number of basis functions: convergence was achieved with respect to the number of the LDA orbitals. The LDA calculation was performed with a plane-wave basis. Non-local norm-conserving pseudopotentials generated by the method developed by Troullier and Martins [85] were used for the LDA, HF and TC calculations. Developing pseudopotentials for solid-state calculations using the TC method is one of the important aspects for the future. Singularities of the electron-electron Coulomb interaction and the Jastrow function in the k-space for the HF and TC methods were handled with a method proposed by Gygi and Baldereschi [74], where we used an auxiliary function of the same form as that proposed by Massidda *et al.* [86]. The Message Passing Interface (MPI) system was used for parallelization of the calculations. The LDA calculations were performed with TAPP code [87, 88], and the HF and TC calculations with TC++ code [24, 25].

The same conditions are used in the whole of this thesis, and so the conditions described here are not mentioned in the later chapters.

3.6 Results: RPA optimization

In this section, we use a Jastrow function without the short-range polynomials, i.e., with $c_{m;\sigma,\sigma'} = 0$ in Eq. (3.1), where the values of A and $C_{\sigma,\sigma'}$ are determined using the RPA in the way described in Section 3.2. The dielectric constants and Jastrow parameter A we used are listed in Table 3.1, which were obtained by extrapolation of the values calculated with about $20 \times 20 \times 20$ to $30 \times 30 \times 30$ k-points. The calculated band gaps are presented in Figure 3.2 and Table 3.2, comparing with those for the HF method, LDA, the experimental values, and the TC method using the Jastrow function Eq. (2.11), with A_0 and $C_{0;\sigma,\sigma'}$, which were determined from the analysis of the homogeneous electron gas. An experimental lattice constant was used for each solid. We used a $4 \times 4 \times 4$ to an $8 \times 8 \times 8$ k-point mesh to have a finite-size error smaller than 0.1eV. We can see that our RPA treatment remedies over-screening caused by A_0, which was determined by an analysis of the uniform electron gas, and the calculated band gaps increased for all materials, compared with the results of the TC method using A_0. In other words, the values of A are smaller than those of A_0 as listed in Table 3.1, so the resulting band gaps slightly approach the HF ($A = 0$) band gaps. In particular, a wide-gap insulator like lithium fluoride is much affected by the RPA treatment, and its band gap is much improved. It is because the electronic structure of such a wide-gap insulator is much different from that of the uniform electron gas, and so the original value A_0 is quite inappropriate. In contrast, the TC method with RPA is found to overestimate the band gaps about 1eV for other

	$\varepsilon_{\rm calc}$	$\varepsilon_{\rm exp}$	A/A_0
Si	13.73	11.9[a]	0.9629
β-SiC	7.213	6.52[a]	0.9281
LiH	4.810	3.6[b]	0.8900
C (diamond)	5.950	5.7[a]	0.9121
LiCl	3.430	2.79[c]	0.8417
LiF	2.117	1.93[c]	0.7264

Table 3.1: Calculated dielectric constants $\varepsilon_{\rm calc}$, experimental values $\varepsilon_{\rm exp}$, and the values of A/A_0 calculated using $\varepsilon_{\rm calc}$. [a] Ref. [41], [b] Ref. [89], [c] Ref. [90].

systems, which are sometimes worse than those obtained from the TC method using the Jastrow function with A_0 and $C_{0;\sigma,\sigma'}$. However, this situation is not surprising because the value of A determined by RPA is not necessarily optimal for short-range description, whereas the parameter A determines the behavior of the Jastrow function in the whole region. Therefore, in the next section, we introduce the short-range polynomials as Eq. (3.1) though we shall also see that such treatment does not yield satisfactory improvement.

Before going to the next section, we mention that the calculated values of the dielectric constants are somewhat different from the experimental values (see Table 3.1.) and such differences change the calculated values of the band gaps a bit, but do not affect our conclusion in this section. For example, the band gaps calculated with A and $C_{\sigma,\sigma'}$, for which values are determined with experimental values of the dielectric constants, are 3.24 eV for β-SiC and 14.4 eV for LiF, which are respectively 0.08 and 0.4 eV larger than those (3.16 and 14.0 eV) from calculated dielectric constants.

3.7 Results: pseudo-variance minimization

Convergence issues

In this section, we apply the pseudo-variance minimization to the optimization of the short-range parameters of the Jastrow function for bulk silicon. Before showing the results for the physical quantities, we present the convergence property of this scheme. Figure 3.3 presents the plot of the convergence of the total energy and the value of the Jastrow parameter $c_{0;\rm para}$ for bulk silicon in terms of the number of conduction bands N_{bc} taken into consideration for the excited configurations in calculating the pseudo-variance. We used $N_k = 4\times4\times4$, $N_{k,mini} = 2\times2\times2$, $N_{bv} = 4$ (full), and $M = 3$ in Eq. (3.1) for these calculations. An experimental lattice constant (10.26 Bohr) [41] was used. The cutoff energy for plane waves was 36 Ry, and the number of LDA orbitals used in expanding the

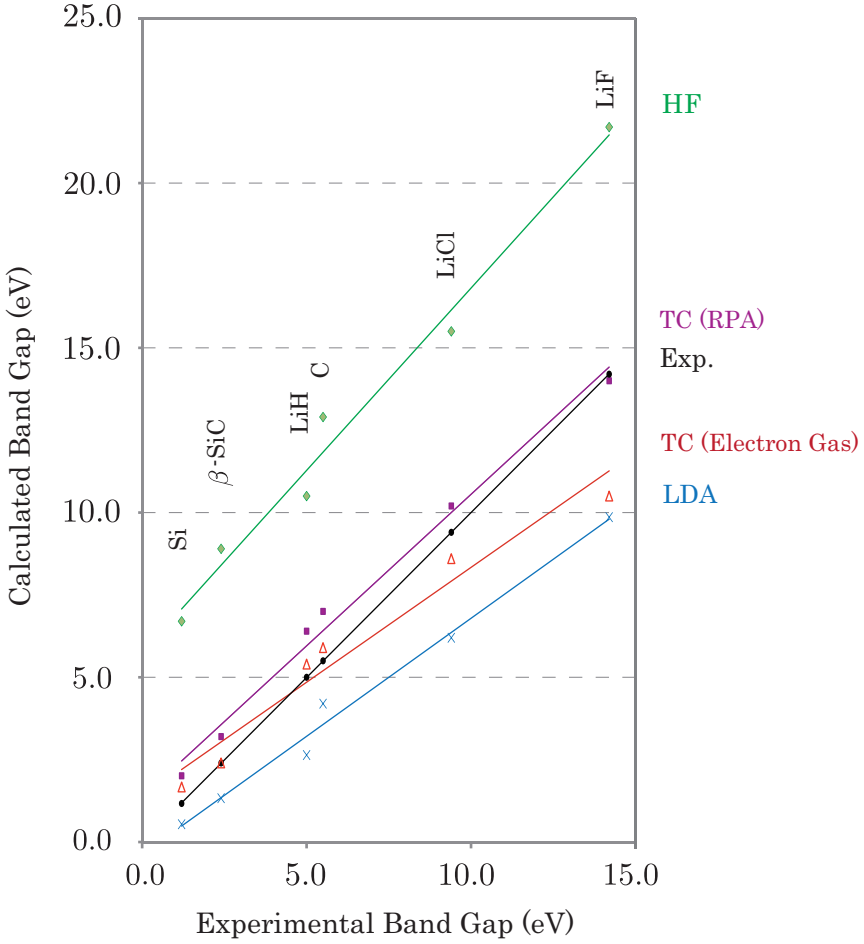

Figure 3.2: Band gaps for several solids calculated with each method. 'TC (Electron Gas)' used a Jastrow function as Eq. (2.11). 'TC (RPA)' used the same form of the Jastrow function, but A_0 and $C_{0;\sigma,\sigma'}$ are replaced with A and $C_{\sigma,\sigma'}$, whose values are determined in the way described in Section 3.2. The lines are drawn as visual guides.

	LDA	TC (Electron Gas)	TC (RPA)	HF	Exp.
Si	0.5[a]	1.7[a]	2.0	6.7[a]	1.17[b]
β-SiC	1.4[a]	2.4[a]	3.2	8.9[a]	2.4[c]
LiH	2.6	5.4	6.4	10.5	5.0[d]
C (diamond)	4.2[a]	5.9[a]	7.0	12.9[a]	5.48[c]
LiCl	6.2	8.6	10.2	15.5	9.4[e]
LiF	9.9	10.5	14.0	21.7	14.2[f]

Table 3.2: Band gaps (eV) for several solids calculated using various methods. 'TC (Electron Gas)' used a Jastrow function of Eq. (2.11). 'TC (RPA)' used the same form of the Jastrow function, but A_0 and $C_{0;\sigma,\sigma'}$ are replaced with A and $C_{\sigma,\sigma'}$, the values of which were determined in the way described in Section 3.2. [a] Ref. [25], [b] Ref. [40], [c] Ref. [41], [d] Ref. [42], [e] Ref. [43], [f] Ref. [44].

one-electron orbitals of the TC method was 100. In Figure 3.3, we can see that reasonable convergence has been achieved with respect to the practical number of conduction bands. In addition, we also investigated convergence in terms of the self-consistent repetition of the Jastrow-factor optimization and orbital optimization as specified in the lower part of Figure 3.1, and verified that it affects results such as the total energy minimally for bulk silicon. For example, differences between results with a self-consistent repetition in Figure 3.1 and those without, i.e., using one-electron orbitals optimized for $u(x, x') = (A/|\mathbf{r}-\mathbf{r}'|)(1-\exp(-|\mathbf{r}-\mathbf{r}'|/C_{\sigma,\sigma'}))$ and the Jastrow function optimized for these orbitals, are about 0.0008 Hartree and 0.0004, for the total energy per primitive cell and the Jastrow parameter $c_{0;\mathrm{para}}$, respectively for $N_{bc} = 48$. (Cf. The total energy and the Jastrow parameter $c_{0;\mathrm{para}}$ calculated without this self-consistent repetition are -7.878 Hartree and 0.0064, respectively.) The minimal change seems to be because an optimized Jastrow function is very similar to the one without short-range polynomials for bulk silicon as we shall see in the next section.

Application to bulk silicon, lithium hydride, and silicon carbide

We investigate how the short-range terms affect some physical quantities using the pseudo-variance minimization for bulk silicon. The whole calculation described in Section 3.4 was performed for several values of M using $N_k = 4 \times 4 \times 4$, $N_{k,mini} = 2 \times 2 \times 2$, $N_{bv} = 4$ (full), and $N_{bc} = 48$. Table 3.3 presents several quantities obtained in our calculations: the indirect and direct band gaps, valence bandwidths, lattice constants, bulk moduli, fraction of the valence correlation energy retrieved within our calculations R_{corr} (%), the values of the pseudo-variances, and computation time for the pseudo-variance minimization using

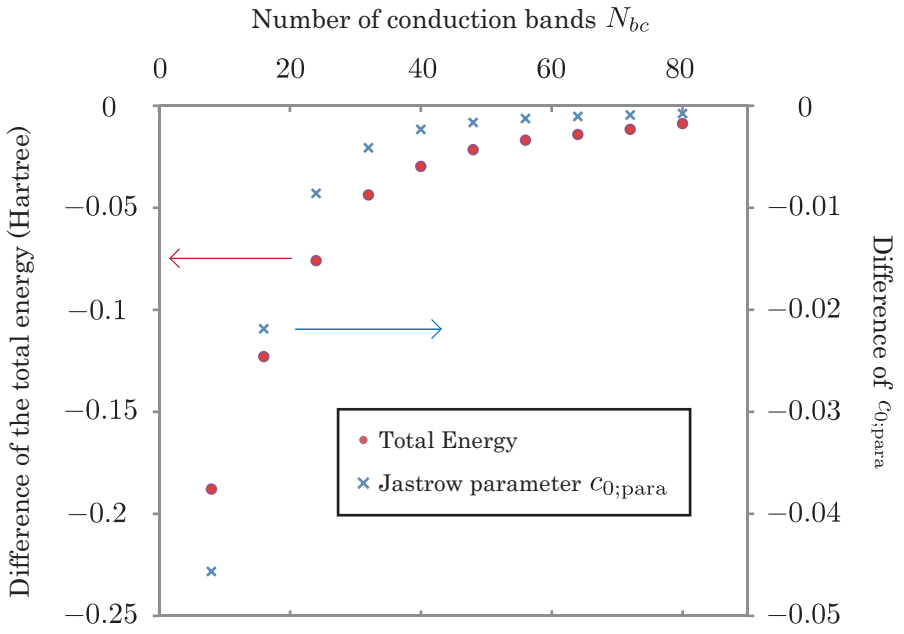

Figure 3.3: Convergence of the total energy per primitive cell and the Jastrow parameter $c_{0;\mathrm{para}}$ is shown for bulk silicon using $N_k = 4 \times 4 \times 4$, $N_{k,mini} = 2 \times 2 \times 2$, $N_{bv} = 4$ (full), and $M = 3$ in Eq. (3.1). Differences in values for the total energy and $c_{0;\mathrm{para}}$ for each N_{bc} from those for $N_{bc} = 196$ (-7.870 Hartree and 0.0107, respectively) are plotted.

64 MPI processes of the K-computer, Kobe, Japan. The pseudo-variance for the HF wave function is defined as in Eq. (3.14) with $\mathcal{H}_{\rm TC} = \mathcal{H}$, i.e., the Jastrow factor $F = 1$. $R_{\rm corr}$ for the total energy E is defined as $100 \times (E_{\rm HF} - E)/(E_{\rm HF,ref} - E_{\rm DMC,ref})$ (%), where $E_{\rm HF}$ is the HF total energy calculated by us, $E_{\rm DMC,ref}$ the DMC total energy using a 54-atom simulation cell obtained from Ref. [75], and $E_{\rm HF,ref}$ the HF total energy from the same reference. In evaluating $R_{\rm corr}$, the total energies for the HF and TC methods are extrapolated in the limit $N_k \to \infty$. For this purpose, we used an approximate relation [25, 91],

$$E_{\rm tot} = E_{\rm tot,inf} + b \times N_k^{-1}, \tag{3.16}$$

where the total energies, $E_{\rm tot}$, corresponding to $N_k = 4 \times 4 \times 4$ and $6 \times 6 \times 6$ are used for solving the SCF equations to obtain an extrapolated value, $E_{\rm tot,inf}$. Whereas the SCF equations here are solved for two different k-point meshes, the Jastrow factor is always optimized using the pseudo-variance minimization with $N_k = 4 \times 4 \times 4$ as mentioned above. For all calculations in this subsection, the cutoff energy for plane waves was 36 Ry and the number of LDA basis orbitals used in expanding the HF or TC orbitals was 100, except for band calculations in the HF method, which was performed using an $8 \times 8 \times 8$ k-point mesh, 25 Ry cutoff energy, and 50 LDA orbitals, and other calculations performed in the references. An experimental lattice constant (10.26 Bohr) was used.

We can see that the pseudo-variance decreases by inclusion of the additional degrees of freedom in the Jastrow factor, and the values corresponding to the TC wave functions are much lower than that for the HF wave function. These results show that the pseudo-variance can be used as a measure of the quality of the wave function, which can be evaluated with reasonable computational cost, though the computational cost is found to be comparable to the QMC calculations. However, the band properties, i.e., the band gaps and valence bandwidth, change very little by inclusion of the short-range terms regardless of their number, M, for bulk silicon. This result suggests that an accurate description of the band properties of bulk silicon requires more elaborate treatment of the electron correlation, e.g., using more general forms of the Jastrow function like $\sum_p w_p(\mathbf{r}) u(\mathbf{r} - \mathbf{r}') w_p(\mathbf{r}')$, or post-HF treatment beyond the single Slater determinant. Fig. 3.4 presents Jastrow functions optimized with various conditions. Jastrow functions for $M \geq 4$ are not depicted here because they are almost indistinguishable with that for $M = 3$. In Fig. 3.4, these functions are almost identical, which means that the original Jastrow function without short-range polynomial terms is a fairly good guess.

We also applied the pseudo-variance minimization and performed similar calculations for lithium hydride and silicon carbide presented in Table 3.4 and Table 3.5, respectively. For calculations of lithium hydride, we used $N_k = 4 \times 4 \times 4$, $N_{k,mini} = 2 \times 2 \times 2$, $N_{bv} = 1$ (full), and $N_{bc} = 48$ for pseudo-variance minimization, and 49 or 64 Ry cutoff energy for plane waves and 100 LDA orbitals to expand one-electron orbitals of the HF and TC

methods. As for silicon carbide, we used $N_k = 4\times4\times4$, $N_{k,mini} = 2\times2\times2$, $N_{bv} = 4$ (full), and $N_{bc} = 48$ for pseudo-variance minimization, and 49 or 64 Ry cutoff energy for plane wave and 200 LDA orbitals to expand one-electron orbitals of the HF and TC methods. For both materials, HF band calculations are carried out using the large number of k-points ($8 \times 8 \times 8$ at most) to obtain enough convergence. In both tables, we can observe the essentially same behavior as bulk silicon, i.e., band energies are not altered so much by inclusion of short-range polynomials. These results reinforce our argument about a role of short-range terms and an effect of pseudo-variance minimization mentioned above for the case of silicon. The direct band gap of silicon carbide slightly decreases when $M = 4$, but we verified that it again increases to 9.4eV for $M = 5$. Moreover, the pseudo-variance decreases by our RPA treatment for our three test cases (silicon, silicon carbide, and lithium hydride) even though the Jastrow parameters A and C are not determined by pseudo-variance minimization. It suggests that our RPA treatment works well for optimization and also the pseudo-variance is a good measure of a quality of the trial wave function.

In conclusion of this chapter, we optimize the Jastrow factor by two ways. First, long-range parameters are determined by using the dielectric constant obtained with RPA calculations. This treatment improves the band gap of a wide-gap insulator, LiF, but the band gaps of other materials are not improved. Next, short-range parameters are optimized by pseudo-variance minimization developed by us. It works with reasonable computational cost, but it is found that band energies are not improved by inclusion of short-range polynomials we used here.

To overcome this situation, we apply the MP2 perturbation theory to the TC Hamiltonian to go beyond a single-Slater-determinant assumption. For this purpose, we should introduce a biorthogonal formulation of the TC method owing to the non-Hermiticity of the TC Hamiltonian. Therefore, in the next chapter, we briefly introduce the biorthogonal formulation of the TC method, and in the following chapter, we apply the MP2 perturbation theory to the TC Hamiltonian.

RPA opt.	no	yes	yes	yes	yes	yes	yes	-	-	-	-
M	0	0	2	3	4	5	6	LDA	HF	DMC	Exp.
Indirect bandgaps (eV)	1.7	2.0	2.1	2.1	2.1	2.1	2.1	0.5[a]	6.7[a]	-	1.17[b]
Direct bandgaps (eV)	4.2	4.6	4.6	4.6	4.6	4.6	4.6	2.6	9.2	3.70[c]	3.40, 3.05[d]
Valence bandwidths (eV)	15.0	15.1	15.1	15.1	15.1	15.1	15.1	11.9[a]	16.8[a]	13.58[c]	12.5(6)[d]
R_{corr} (%)	114	109	71	72	73	71	70	90[a]	0	-	-
σ^2_{PS} (10^{-3}Hartree^2)	6.82	6.34	4.61	4.54	4.53	4.49	4.40	-	54.1	-	-
Computation time (hours)	-	-	0.9	1.6	2.8	4.2	6.0	-	-	-	-

Table 3.3: Indirect and direct band gaps, valence bandwidths, fraction of the valence correlation energy retrieved within our calculations (compared with the result from the fixed-node DMC calculation of Ref. [75] using a 54-atom simulation cell) R_{corr} (%), the values of the pseudo-variances, and computation time for pseudo-variance minimization using 64 MPI processes of the K-computer, Kobe, Japan, for bulk silicon calculated with each type of the Jastrow function. See the main text for the definition of R_{corr}. $M = 0$ corresponds to the Jastrow function without short-range polynomials. [a] Ref. [25], [b] Ref. [40], [c] Ref. [35], [d] From the compilation given in Ref. [92].

RPA opt.	no	yes	yes	yes	yes	-	-	-
M	0	0	2	3	4	LDA	HF	Exp.
Direct bandgaps (eV)	5.4	6.4	6.4	6.5	6.7	2.6	10.5	5.0[a]
Valence bandwidths (eV)	6.7	6.8	6.8	6.7	6.6	5.5	7.5	6.3±1.1[b]
σ^2_{PS} (10^{-4}Hartree^2)	11.87	10.54	8.54	8.34	8.20	-	114.5	-

Table 3.4: Band properties of lithium hydride calculated with several conditions for the Jastrow function just as Table 3.3. [a] Ref. [42], [b] Ref. [93].

RPA opt.	no	yes	yes	yes	yes	-	-	-
M	0	0	2	3	4	LDA	HF	Exp.
Indirect bandgaps (eV)	2.4[a]	3.2	3.3	3.2	3.2	1.4[a]	8.9[a]	2.4[b]
Direct bandgaps (eV)	8.5	9.3	9.5	9.5	8.9	6.4	15.4	6.0[c]
Valence bandwidths (eV)	19.4	19.6	19.6	19.6	19.6	15.3	21.3	-
σ^2_{PS} (10^{-3}Hartree^2)	17.34	14.48	10.78	10.64	10.59	-	88.8	-

Table 3.5: Band properties of silicon carbide calculated with several conditions for the Jastrow function just as Table 3.3. [a] Ref. [25], [b] Ref. [41], [c] Ref. [94].

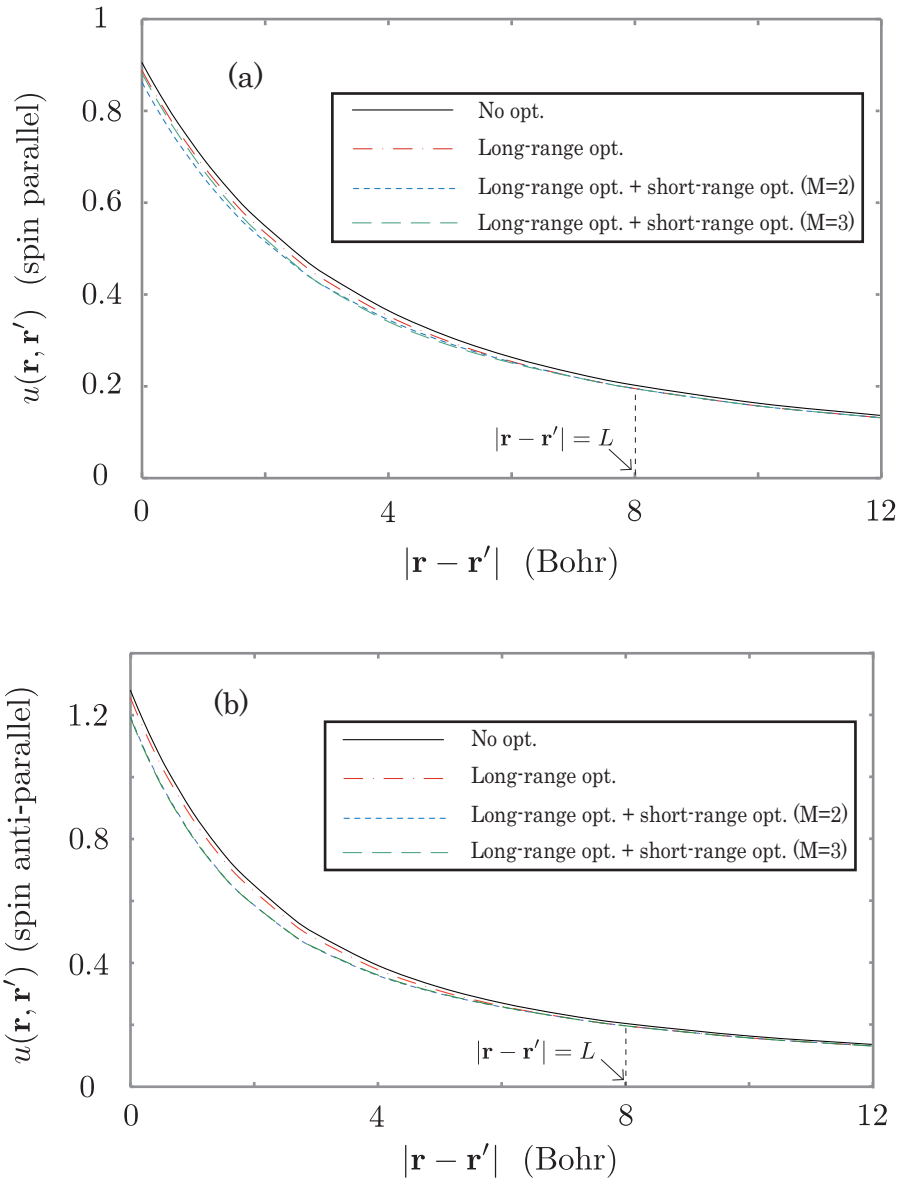

Figure 3.4: Jastrow functions for parallel (a) and anti-parallel (b) spins optimized with various conditions. The solid black line plots the Jastrow function without optimization, i.e., Eq. (2.11), the dot-dash red line the same form of the Jastrow function where A_0 and $C_{0;\sigma,\sigma'}$ are replaced with A and $C_{\sigma,\sigma'}$, whose values are determined in the manner described in Section 3.2, the short-dashed blue line the Jastrow function as in Eq. (3.1) with $M = 2$, and the long-dashed green line one with $M = 3$.

Chapter 4

Biorthogonal formulation of the TC method (BiTC method)

To apply the MP2 perturbation theory to the TC method, we should introduce a biorthogonal formulation of the TC method, called the BiTC method. The BiTC method was already developed and applied to the molecular systems [95], but not yet to the periodic systems like solids. In this chapter, we introduce the BiTC method and show our results of its application to solid-state calculations.

4.1 Formalism of the BiTC method

In the biorthogonal formulation of the TC method, we assume Slater determinants $X = (1/\sqrt{N!})\det[\chi_i(x_j)]$ and $\Phi = (1/\sqrt{N!})\det[\phi_i(x_j)]$ are left and right eigenstates of the TC Hamiltonian, respectively. The total energy is evaluated as $\mathrm{Re}[\langle X|\mathcal{H}_{TC}|\Phi\rangle]$, and an SCF equation for the BiTC method is

$$\begin{aligned}
&\left(-\frac{1}{2}\nabla_1^2 + v_{\mathrm{ext}}(x_1)\right)\phi_i(x_1) \\
&+\sum_{j=1}^{N}\int \mathrm{d}x_2\ \chi_j^*(x_2)\Bigg(\frac{1}{|\mathbf{r}_1-\mathbf{r}_2|} + \frac{1}{2}\big(\nabla_1^2 u(x_1,x_2) + \nabla_2^2 u(x_1,x_2) \\
&-(\nabla_1 u(x_1,x_2))^2 - (\nabla_2 u(x_1,x_2))^2\big) + \nabla_1 u(x_1,x_2)\cdot\nabla_1 + \nabla_2 u(x_1,x_2)\cdot\nabla_2\Bigg) \\
&\times\det[\phi_{i,j}(x_{1,2})] - \frac{1}{2}\sum_{j=1}^{N}\sum_{k=1}^{N}\int \mathrm{d}x_2\mathrm{d}x_3\ \chi_j^*(x_2)\chi_k^*(x_3) \\
&\times\big(\nabla_1 u(x_1,x_2)\cdot\nabla_1 u(x_1,x_3) + \nabla_2 u(x_2,x_1)\cdot\nabla_2 u(x_2,x_3) + \nabla_3 u(x_3,x_1)\nabla_3 u(x_3,x_2)\big) \\
&\times\det[\phi_{i,j,k}(x_{1,2,3})] = \epsilon_i\phi_i(x_1),
\end{aligned} \tag{4.1}$$

where the one-electron orbitals for the left determinant, $\chi(x)$, are biorthogonal to those for the right determinant, $\phi(x)$:

$$\int \mathrm{d}x\ \chi_i^*(x)\phi_j(x) = \delta_{ij}, \tag{4.2}$$

and normalization condition we use is

$$\int \mathrm{d}x\ \phi_i^*(x)\phi_i(x) = 1. \tag{4.3}$$

In the original formalism of the TC method, ϵ_{ij} on the right-hand side of the SCF equation Eq. (2.10) is not diagonalized (i.e., ϵ_{ij} for $i \neq j$ are not necessarily zero) because the one-electron orbitals is orthogonalized and so are not the eigenstates of the TC-Fock operator. On the other hand, ϵ_{ij} is diagonalized (i.e., $\epsilon_{ij} = 0$ for $i \neq j$ and rename the diagonal elements ϵ_{ii} as ϵ_i) in the BiTC-SCF equation Eq. (4.1). This is because the right and left eigenstates of the general linear operator can be biorthogonalized.

4.2 Differences between the TC and BiTC methods

Differences between the TC and BiTC methods are summarized in Table 4.1. Orthogonality among the one-electron orbitals, diagonalization of ϵ_{ij}, and evaluation of the total energy are mentioned in the previous section. Koopmans' theorem is proved for the TC method in Ref. [23], and that for the BiTC method can be verified in the same manner. Hellmann-Feynman theorem [96, 97] states

$$\frac{\mathrm{d}E_\lambda}{\mathrm{d}\lambda} = \langle\Phi_\lambda|\frac{\mathrm{d}\mathcal{H}_\lambda}{\mathrm{d}\lambda}|\Phi_\lambda\rangle, \tag{4.4}$$

where λ is a general parameter and is usually coordinates of the nucleus, and the left eigenstate should be replaced with X for the BiTC method. Impressive feature of this theorem is that $\mathrm{d}\Phi_\lambda/\mathrm{d}\lambda$ does not appear on the right-hand side, which enables one to explore the stable structures of systems easily. However, for the conventional TC method, this theorem does not hold owing to the fact that $\langle\Phi_\lambda|$ is *not* the left eigenstate of the Hamiltonian. There is no such problem for the BiTC method, which enables one to optimize the crystal structure using the Hellman-Feynman force defined as the above equation, and is one of the great advantages of the BiTC method. Brillouin's theorem is mentioned and proved in Appendix A, and is utilized in the MP2 perturbation theory (Chapter 5) and CIS method (Chapter 6). We shall see that the biorthogonal formulation is required for applying the MP2 perturbation theory to the TC method in Chapter 5.

In addition to this table, computational cost for the BiTC method is about 1.5 times as expensive as that for the TC method because some Hermitian terms in the TC method can be evaluated with small computational cost (e.g., for arbitrary Hermitian operator

	TC method	BiTC method
Orthogonality	$\langle\phi_i\|\phi_j\rangle = \delta_{ij}$	$\langle\chi_i\|\phi_j\rangle = \delta_{ij}$, $\langle\phi_i\|\phi_i\rangle = 1$
Eigenvalues ϵ_{ij}	not diagonalized	diagonalized
Koopmans' theorem	holds for $\mathrm{Re}[\epsilon_{ii}]$	
Total energy	$\mathrm{Re}[\langle\Phi\|\mathcal{H}_{TC}\|\Phi\rangle]/\langle\Phi\|\Phi\rangle]$	$\mathrm{Re}[\langle X\|\mathcal{H}_{TC}\|\Phi\rangle]/\langle X\|\Phi\rangle]$
Hellmann-Feynman theorem	does not hold	holds
Brillouin's theorem	partially holds	holds
	$(\langle\Phi_i^a\|\mathcal{H}_{TC}\|\Phi_0\rangle = 0)$	$(\langle X_0\|\mathcal{H}_{TC}\|\Phi_i^a\rangle = \langle X_i^a\|\mathcal{H}_{TC}\|\Phi_0\rangle = 0)$
MP perturbation theory	not applicable	applicable
	(in the regular manner)	

Table 4.1: Differences between the TC and BiTC methods.

$\hat{h}$, $\langle\phi_i|\hat{h}|\phi_j\rangle = (\langle\phi_j|\hat{h}|\phi_i\rangle)^*$ can be utilized, but $\langle\chi_i|\hat{h}|\phi_j\rangle \neq (\langle\chi_j|\hat{h}|\phi_i\rangle)^*$.). Also, memory requirements are higher for the BiTC method than for the TC method owing to the necessity to store both ϕ and χ.

4.3 Results: band gaps and total energies

The TC and BiTC methods have many differences as we have seen in the previous section, and so the calculation results of the physical quantities such as the band gaps can differ. Table 4.2 presents the calculated band gaps using the TC and BiTC methods. For silicon, lithium hydride, and diamond, the band gaps do not differ so much between the TC and BiTC methods, but other materials, especially lithium fluoride, show not small differences. This is because we use different formalisms, i.e., solve different SCF equations, between these two methods. Comparing with experimental results, the BiTC method shows systematic overestimation of the band gaps. In the next chapter, we consider the MP2 correction to the band energies calculated with the BiTC method to improve this situation.

For bulk silicon, we further checked the differences between the TC and BiTC methods in detail. Table 4.3 presents some kinds of physical quantities calculated using the TC and BiTC methods. We can see that all quantities listed here are very similar between these two methods.

	TC	BiTC	Experiment
Si	2.0	2.2	1.17[a]
β-SiC	3.2	3.9	2.4[b]
LiH	6.4	6.4	5.0[c]
C (diamond)	7.0	7.1	5.5[b]
LiCl	10.2	11.0	9.4[d]
LiF	14.0	17.1	14.2[e]

Table 4.2: Calculated band gaps (eV) using the TC and BiTC methods. [a] Ref. [40], [b] Ref. [41], [c] Ref. [42], [d] Ref. [43], [e] Ref. [44].

	TC	BiTC	Experiment
Indirect band gaps (eV)	2.0	2.2	1.17[a]
Direct band gaps at the Gamma point (eV)	4.6	4.6	3.40, 3.05[b]
Valence bandwidths (eV)	15.1	15.1	12.5(6)[b]
a (Bohr)	10.08	10.09	10.24(10.26)[c]
B (GPa)	113	113	101(99)[c]
Valence correlation energies retrieved (%)	109	110	-

Table 4.3: Several physical quantities of bulk silicon calculated using the TC and BiTC methods. Valence correlation energy retrieved is defined in Chapter 3. The experimental lattice constant and bulk modulus are corrected for zero-point vibrational effects and those in parentheses correspond to uncorrected experimental values. [a] Ref. [40], [b] From the compilation given in Ref. [92], [c] Ref. [98] and references therein.

Chapter 5

The second-order Møller-Plesset (MP2) perturbation theory

Using the biorthogonal formalism of the TC method introduced in the previous chapter, we apply the MP2 perturbation theory to the TC Hamiltonian. Band structure calculations by using the BiTC-MP2 method are presented.

5.1 MP2 perturbation theory for the HF method

We briefly review the conventional MP2 perturbation theory applied to the HF method [15]. In the MP2 perturbation theory, Hamiltonian is divided into two parts,

$$\mathcal{H} = \mathcal{H}_0 + V, \tag{5.1}$$

where $\mathcal{H}_0 = \sum_i \hat{h}(x_i)$ and $\hat{h}(x_i)$ is the HF-Fock operator appeared in the SCF equation of the HF method, Eq. (1.5). V is defined as $\mathcal{H} - \mathcal{H}_0$. Here we apply the many-body perturbation theory to this partitioning of the Hamiltonian. (V is treated as the perturbation term.) The ground state is assumed not to be degenerated here.

Unperturbed (zeroth-order) state and energy

Because $\hat{h}(x)\phi_i(x) = \epsilon_i\phi_i(x)$ holds for each orbital ϕ_i, the Slater determinant, i.e., the HF wave function $\Phi_0 = (1/\sqrt{N!})\det[\phi_{1,\ldots,N}(x_{1,\ldots,N})]$, is the eigenstate of $\mathcal{H}_0$. The zeroth-order contribution of the total energy is $E_{\mathrm{HF}}^{(0)} = \sum_i \epsilon_i$, which is the eigenvalue of the $\mathcal{H}_0$ corresponding to its eigenstate Φ_0.

First-order contribution

The first-order contribution of the total energy $E_{\rm HF}^{(1)}$ is calculated as

$$E_{\rm HF}^{(1)} = \langle \Phi_0 | V | \Phi_0 \rangle = E_0 - \sum_i \epsilon_i, \tag{5.2}$$

where E_0 is the HF total energy of the ground state, $\langle \Phi_0 | \mathcal{H} | \Phi_0 \rangle$. Therefore, the HF total energy E_0 equals to $E_{\rm HF}^{(0)} + E_{\rm HF}^{(1)}$.

Second-order contribution

The second-order contribution of the total energy $E_{\rm HF}^{(2)}$ is calculated as

$$E_{\rm HF}^{(2)} = -\sum_{i \neq 0} \frac{|\langle \Phi_i | V | \Phi_0 \rangle|^2}{E_i - E_0}, \tag{5.3}$$

where Φ_i and E_i are the eigenstates and the corresponding eigenvalues of $\mathcal{H}_0$, respectively. The summation runs over all the eigenstates of $\mathcal{H}_0$ except Φ_0.

To calculate Eq. (5.3), we can easily verify that only doubly-excited configurations $\Phi_{i,j}^{a,b} = (1/\sqrt{N!}) \det[\phi_{1,2,\ldots,\hat{i},\ldots,\hat{j},\ldots,N-1,N,a,b}(x_{1,\ldots,N})]$, where electrons belonging to the i- and j-th occupied states are excited to the a- and b-th unoccupied states, can have non-zero contribution to $E_{\rm HF}^{(2)}$ [15]. Therefore, $E^{(2)}$ can be rewritten as

$$E_{\rm HF}^{(2)} = -\sum_{i<j}^{\rm occup} \sum_{a<b}^{\rm unocc} \frac{|\langle a,b||i,j\rangle|^2}{\epsilon_a + \epsilon_b - \epsilon_i - \epsilon_j}, \tag{5.4}$$

where

$$\langle a,b||i,j\rangle \equiv \int {\rm d}x_1 {\rm d}x_2 \; \phi_a^*(x_1)\phi_b^*(x_2) \frac{1}{|\mathbf{r}_1 - \mathbf{r}_2|} \det[\phi_{i,j}(x_{1,2})]. \tag{5.5}$$

This is called the MP2 theory, which is known as a simple but efficient and powerful method for calculating more accurate electronic structure of molecular systems than the HF method. However, for solid-state calculations, the MP2 theory is known to provide inaccurate band gaps for narrow-gap systems, e.g., Si and β-SiC exhibit metallic band structures [51] (also, see our results presented later in this chapter). It seems to be because the starting point of this perturbation, the HF-Fock operator, is much inaccurate for describing the electronic structure in solids. In particular, the screening effect, which is considered to be retrieved with the infinite series of the diagrams like the ring diagrams of RPA, is difficult to take into account by the second-order perturbation, especially for the narrow-gap semiconductors where the dielectric constants are large and perturbation is considered to converge slowly with respect to the order of the perturbation series. To overcome this problem, we apply the MP2 theory to the BiTC method, which is considered to be better starting point than the HF method, for solid-state calculations.

5.2 MP2 perturbation theory for the BiTC method

MP perturbation theory can be applied to the TC Hamiltonian in the similar manner to that for the HF method, as described and applied to molecular systems in Refs. [21, 95]. However, we should use the biorthogonal formalism for the TC method to derive the similar relations to the HF-MP2 method because of the non-Hermiticity of the TC Hamiltonian.

The MP2 correlation energy for the ground state of the BiTC method [95] is

$$E^{(2)}_{\rm BiTC} = -{\rm Re}\Bigg[\sum_{i<j}^{\rm occup} \sum_{a<b}^{\rm unocc} \frac{\langle X_0|\mathcal{H}_{\rm TC}|\Phi^{a,b}_{i,j}\rangle\langle X^{a,b}_{i,j}|\mathcal{H}_{\rm TC}|\Phi_0\rangle}{\epsilon_a+\epsilon_b-\epsilon_i-\epsilon_j} + \sum_{i<j<k}^{\rm occup} \sum_{a<b<c}^{\rm unocc} \frac{\langle X_0|\mathcal{H}_{\rm TC}|\Phi^{a,b,c}_{i,j,k}\rangle\langle X^{a,b,c}_{i,j,k}|\mathcal{H}_{\rm TC}|\Phi_0\rangle}{\epsilon_a+\epsilon_b+\epsilon_c-\epsilon_i-\epsilon_j-\epsilon_k} \Bigg] \tag{5.6}$$

where i, j, k and a, b, c denote occupied and unoccupied one-electron states respectively, and $\Phi^{a,b,c}_{i,j,k}$ and $X^{a,b,c}_{i,j,k}$ are triply excited configurations.

We can see that the Brillouin's theorem for the TC Hamiltonian [95] makes the contribution from singly excited configurations zero just like the HF-MP2 method. However, there are some differences between the BiTC-MP2 and HF-MP2 methods. First, non-Hermiticity of the TC Hamiltonian requires the biorthogonal formulation, and so two kinds of one-electron orbitals (ϕ and χ) appear and the above equation includes complex numbers. Second, the three-body terms are included in the TC Hamiltonian, and then, (i) the contribution from triply excited configurations is non-zero, and (ii) also the contribution from doubly excited configurations involves three-body terms. This situation is similar to that for the pseudo-variance described in Chapter 3, and in this thesis, we ignore the contribution (i), i.e., the second term on the right-hand side in Eq. (5.6) just as in Chapter 3 because of computational cost. Moreover, the contribution from triply excited configurations is expected to be small because one- or two-body operators in the TC Hamiltonian cannot have non-zero contribution for these configurations and also an important contribution of the three-body terms as described in Chapter 3 (Eq. (3.7)) does not appear here.

Then, the total energy we used in this thesis can be rewritten as

$$E^{(2)}_{\rm BiTC} = -{\rm Re}\Bigg[\sum_{i<j}^{\rm occup} \sum_{a<b}^{\rm unocc} \frac{\langle i,j||a,b\rangle_{\rm TC}\langle a,b||i,j\rangle_{\rm TC}}{\epsilon_a+\epsilon_b-\epsilon_i-\epsilon_j} \Bigg], \tag{5.7}$$

where

$$\langle p,q||r,s\rangle_{\rm TC} \equiv \int {\rm d}x_1{\rm d}x_2\ \chi^*_p(x_1)\chi^*_q(x_2)v_{\rm 2body}(x_1,x_2){\rm det}[\phi_{r,s}(x_{1,2})] - \frac{1}{2}\sum_m^{\rm occup} \int {\rm d}x_1{\rm d}x_2{\rm d}x_3\ \chi^*_p(x_1)\chi^*_q(x_2)\chi^*_m(x_3)v_{\rm 3body}(x_1,x_2,x_3){\rm det}[\phi_{r,s,m}(x_{1,2,3})], \tag{5.8}$$

and $v_{2\text{body}}(x_1, x_2)$ and $v_{3\text{body}}(x_1, x_2, x_3)$ are defined as

$$v_{2\text{body}}(x_1, x_2) \equiv \frac{1}{|\mathbf{r}_1 - \mathbf{r}_2|} + \frac{1}{2}\big(\nabla_1^2 u(x_1, x_2) + \nabla_2^2 u(x_1, x_2) - (\nabla_1 u(x_1, x_2))^2 - (\nabla_2 u(x_1, x_2))^2\big) + \nabla_1 u(x_1, x_2) \cdot \nabla_1 + \nabla_2 u(x_1, x_2) \cdot \nabla_2, \tag{5.9}$$

and

$$v_{3\text{body}}(x_1, x_2, x_3) \equiv \nabla_1 u(x_1, x_2) \cdot \nabla_1 u(x_1, x_3) + \nabla_2 u(x_2, x_1) \cdot \nabla_2 u(x_2, x_3) + \nabla_3 u(x_3, x_1) \cdot \nabla_3 u(x_3, x_2). \tag{5.10}$$

5.3 Band correction calculated by the MP2 perturbation theory

By using the MP2 theory, one can also calculate the correction of the band structure, i.e., one-electron energy ϵ_i. For the HF-MP2 method, the below equations can be seen in several articles [99, 51],

$$\epsilon_v^{\text{HF}-\text{MP2}} = \epsilon_v - \sum_{i}^{\text{occup}} \sum_{a<b}^{\text{unocc}} \frac{\langle i, v||a, b\rangle \langle a, b||i, v\rangle}{\epsilon_a + \epsilon_b - \epsilon_i - \epsilon_v} + \sum_{i<j}^{\text{occup}} \sum_{a}^{\text{unocc}} \frac{\langle i, j||a, v\rangle \langle a, v||i, j\rangle}{\epsilon_a + \epsilon_b - \epsilon_i - \epsilon_v}, \tag{5.11}$$

$$\epsilon_c^{\text{HF}-\text{MP2}} = \epsilon_c - \sum_{i}^{\text{occup}} \sum_{a<b}^{\text{unocc}} \frac{\langle i, c||a, b\rangle \langle a, b||i, c\rangle}{\epsilon_a + \epsilon_b - \epsilon_i - \epsilon_c} + \sum_{i<j}^{\text{occup}} \sum_{a}^{\text{unocc}} \frac{\langle i, j||a, c\rangle \langle a, c||i, j\rangle}{\epsilon_a + \epsilon_c - \epsilon_i - \epsilon_j}, \tag{5.12}$$

for the valence band v and conduction band c respectively, and for the BiTC-MP2 method,

$$\epsilon_v^{\text{BiTC}-\text{MP2}} = \epsilon_v - \sum_{i}^{\text{occup}} \sum_{a<b}^{\text{unocc}} \frac{\langle i, v||a, b\rangle_{\text{TC}} \langle a, b||i, v\rangle_{\text{TC}}}{\epsilon_a + \epsilon_b - \epsilon_i - \epsilon_v} + \sum_{i<j}^{\text{occup}} \sum_{a}^{\text{unocc}} \frac{\langle i, j||a, v\rangle_{\text{TC}} \langle a, v||i, j\rangle_{\text{TC}}}{\epsilon_a + \epsilon_b - \epsilon_i - \epsilon_v} + \sum_{i<j}^{\text{occup}} \sum_{a<b}^{\text{unocc}} \left(\frac{1}{2} \frac{\langle i, j||a, b\rangle_{\text{TC}} \langle a, b, v||i, j, v\rangle_3 + \langle i, j, v||a, b, v\rangle_3 \langle a, b||i, j\rangle_{\text{TC}}}{\epsilon_a + \epsilon_b - \epsilon_i - \epsilon_j} + \frac{1}{4} \frac{\langle i, j, v||a, b, v\rangle_3 \langle a, b, v||i, j, v\rangle_3}{\epsilon_a + \epsilon_b - \epsilon_i - \epsilon_j} \right), \tag{5.13}$$

$$\epsilon_c^{\text{BiTC}-\text{MP2}} = \epsilon_c - \sum_{i}^{\text{occup}} \sum_{a<b}^{\text{unocc}} \frac{\langle i, c||a, b\rangle_{\text{TC}} \langle a, b||i, c\rangle_{\text{TC}}}{\epsilon_a + \epsilon_b - \epsilon_i - \epsilon_c} + \sum_{i<j}^{\text{occup}} \sum_{a}^{\text{unocc}} \frac{\langle i, j||a, c\rangle_{\text{TC}} \langle a, c||i, j\rangle_{\text{TC}}}{\epsilon_a + \epsilon_c - \epsilon_i - \epsilon_j} + \sum_{i<j}^{\text{occup}} \sum_{a<b}^{\text{unocc}} \left(\frac{1}{2} \frac{\langle i, j||a, b\rangle_{\text{TC}} \langle a, b, c||i, j, c\rangle_3 + \langle i, j, c||a, b, c\rangle_3 \langle a, b||i, j\rangle_{\text{TC}}}{\epsilon_a + \epsilon_b - \epsilon_i - \epsilon_j} - \frac{1}{4} \frac{\langle i, j, c||a, b, c\rangle_3 \langle a, b, c||i, j, c\rangle_3}{\epsilon_a + \epsilon_b - \epsilon_i - \epsilon_j} \right), \tag{5.14}$$

where

$$\langle p,q,r||s,t,u\rangle_3 \equiv \int \mathrm{d}x_1\mathrm{d}x_2\mathrm{d}x_3\ \chi_p^*(x_1)\chi_q^*(x_2)\chi_r^*(x_3)v_{3\mathrm{body}}(x_1,x_2,x_3)\det[\phi_{s,t,u}(x_{1,2,3})]. \tag{5.15}$$

These equations are derived by calculating the difference between the total energies of the system of N and $N \pm 1$ electrons.

5.4 Computational cost

The HF-MP2 method requires the computational cost of $\mathcal{O}(N_k^3 N_{bv}^2 N_{bc}^2 N_{pw})$ when ones use the plane waves for calculations. This cost comes from the fact that the number of the possible combinations of the indices i, j, a, and b in Eq. (5.4) is $N_k^3 N_{bv}^2 N_{bc}^2$ because of the conservation law of the crystal momentum. To calculate the band correction described in the previous section, $N_{bv}^2 N_{bc}^2$ is replaced with $N_{bv}N_{bc}^3 + N_{bv}^2 N_{bc}^2 + N_{bv}^3 N_{bc}$.

As for the BiTC-MP2 method, the computational cost including the three-electron excitation (Eq. (5.6)) is $\mathcal{O}(N_k^5 N_{bv}^3 N_{bc}^3 N_{pw})$, which is extremely expensive and intractable. When we neglect the three-electron excitation as described in Section 5.2, the MP2 correlation energy (Eq. (5.7)) requires the computational cost of $\mathcal{O}(N_k^3 N_{bv}^2 N_{bc}^2 N_{pw})$, which is the same order as that of the HF-MP2 method. It is remarkable feature that the three-body potentials included in Eq. (5.7) can be calculated with the same computational cost as that for the two-body potentials using the similar technique to that for solving the TC-SCF equation [25]. Moreover, as we shall see in the following sections, the amount of the BiTC-MP2 correlation energy is much smaller than that for the HF-MP2 method, which enables faster convergence with respect to the parameter such as the number of k-points, and so rather lower computational cost is required for the BiTC-MP2 method than for the HF-MP2 method in some cases.

Additionally, we should note that computational cost required for calculating the last two lines of Eqs. (5.13) and (5.14) is a bit expensive: $\mathcal{O}(N_k^3 N_{bv}^2 N_{bc}^2 N_{pw})$ for *each* ϵ_v or ϵ_c, which is larger than computational cost of remaining terms. However, we verified that contribution of these expensive terms is small: less than 0.1 eV for all calculations performed in this thesis. Therefore, we can neglect the last two lines of Eqs. (5.13) and (5.14) with small error while we did not do so in this thesis.

5.5 Results: convergence issues

In this section, we investigate the convergence issues of the MP2 correlation energy with respect to the number of conduction bands and k-points. This issue largely affects whether calculations can be carried out with practical computational cost because computation time increases rapidly as the number of these parameters become larger.

Figure 5.1 presents the plot of convergence of the MP2 correlation energy with respect to the number of conduction bands, N_{bc}, for lithium hydride. We used a $3 \times 3 \times 3$ k-point mesh, one (full) valence band, 36 Ry for the cutoff energy for plane waves, and 100 LDA orbitals for each k-point in expanding the one-electron orbitals of the HF and BiTC methods.

We can see several interesting features here. First, the MP2 correlation energy can be well extrapolated with a linear function of the inverse of the number of the conduction bands both for the HF-MP2 and BiTC-MP2 methods. This is an advantageous feature in terms of computational cost because calculations involving a very large number of the conduction bands are not necessary. The reason why such a linear behavior is observed is essentially the same as the reason explained in Ref. [100]. Second, the MP2 correlation energy of the BiTC-MP2 method is much smaller than that of the HF-MP2 method, which is also advantageous for the BiTC-MP2 method with respect to computational cost because convergence is easily achieved comparing with the HF-MP2 method. This feature comes from the fact that a large part of the correlation energy is already retrieved at the level of the BiTC calculation. Actually, the correlation energy per primitive cell retrieved with the BiTC method is -0.05 Hartree, which is a similar amount to the HF-MP2 correlation energy seen in Figure 5.1, about -0.04 Hartree, which is also considered to be a major part of the correlation energy. Finally, the MP2 correlation energy can be positive for the BiTC-MP2 method while that for the HF-MP2 method is always negative (cf., Eq. (5.4)).

Figure 5.2 presents the plot of convergence of the MP2 band corrections to the valence-band minimum and conduction-band minimum at the Γ point with respect to the number of conduction bands for bulk silicon. Those are relative values to the MP2 band corrections to the valence-band maximum at the Γ point, which are set to zero. We used a $2 \times 2 \times 2$ k-point mesh, four (full) valence bands, 25 Ry for the cutoff energy for plane waves, and 100 LDA orbitals for each k-point in expanding the one-electron orbitals of the HF and BiTC methods. We can see that the MP2 corrections to the BiTC-MP2 method are smaller than those for the HF-MP2 method similarly to the case of the total energy as seen above. In addition, it is easier for the BiTC-MP2 method to achieve enough convergence than for the HF-MP2 method, and linear extrapolation can work for both methods. We also checked convergence of the MP2 band corrections to the band gap of lithium hydride with respect to the number of conduction bands, which is presented in Figure 5.3. We used a $2 \times 2 \times 2$ k-point mesh, one (full) valence bands, 36 Ry for the cutoff energy for plane waves, and 200 LDA orbitals for each k-point in expanding the one-electron orbitals of the HF and BiTC methods. For this material, values of the MP2 band correction show oscillating behavior both for the HF-MP2 and BiTC-MP2 methods, but for large values of the number of conduction bands, linear extrapolation is still valid. In calculations using a large number of k-points in the following sections, it is sometimes difficult in terms of

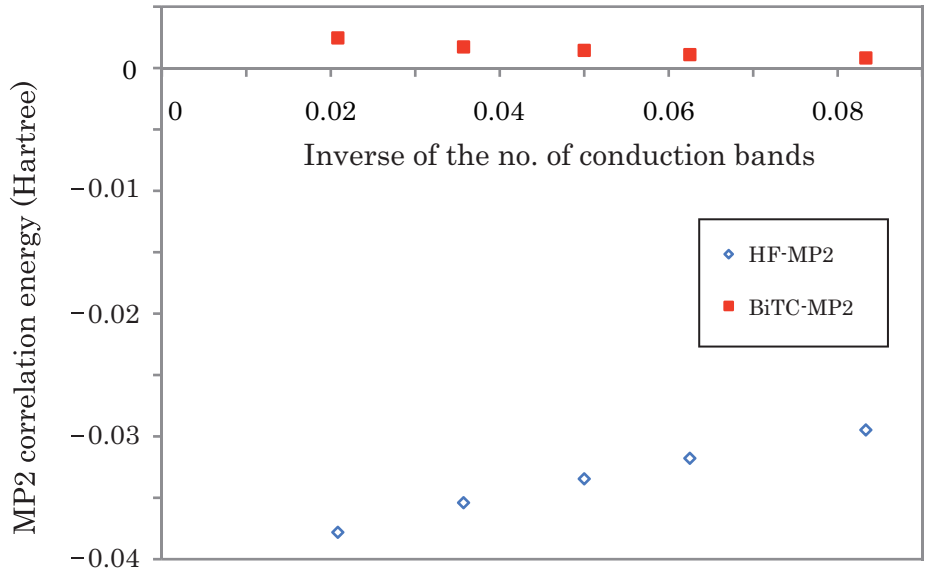

Figure 5.1: MP2 correlation energy per primitive cell of lithium hydride calculated using the HF-MP2 and BiTC-MP2 methods.

computational cost to take a sufficiently large number of the conduction bands. In some cases, we adopt the MP2 correction corresponding to a small number of the conduction bands if oscillation as observed in Figure 5.3 is verified and the MP2 correction of the chosen N_{bc} is considered to be near that for $N_{bc} \to \infty$.

Next, we investigate convergence with respect to the number of k-points, N_k. Figure 5.4 presents the plot of convergence of the MP2 band corrections to the direct band gap at the Γ point with respect to the number of k-points for silicon. We used four (full) valence band, 25 Ry for the cutoff energy for plane waves, and 100 LDA orbitals for each k-point in expanding the one-electron orbitals of the HF and BiTC methods. Contribution from 8 and 12 conduction bands was calculated for the HF-MP2 and BiTC-MP2 methods, respectively. It is difficult to find some simple relationship between the number of k-points and the corresponding values of the MP2 corrections for extrapolation to $N_k \to \infty$ limit. However, the number of k-points largely affects the MP2 corrections and MP2 calculations using a large N_k are enormously expensive. Therefore, in this thesis, we assumed that the MP2 band correction is approximately a linear or quadratic function of the inverse of the number of k-points for large N_k, and calculated the extrapolated value of the MP2 band correction corresponding to $N_k \to \infty$ limit. For band structure calculations, we did not use the data corresponding to a $2 \times 2 \times 2$ k-point mesh for extrapolation because our extrapolation is not expected to work well for such a small N_k.

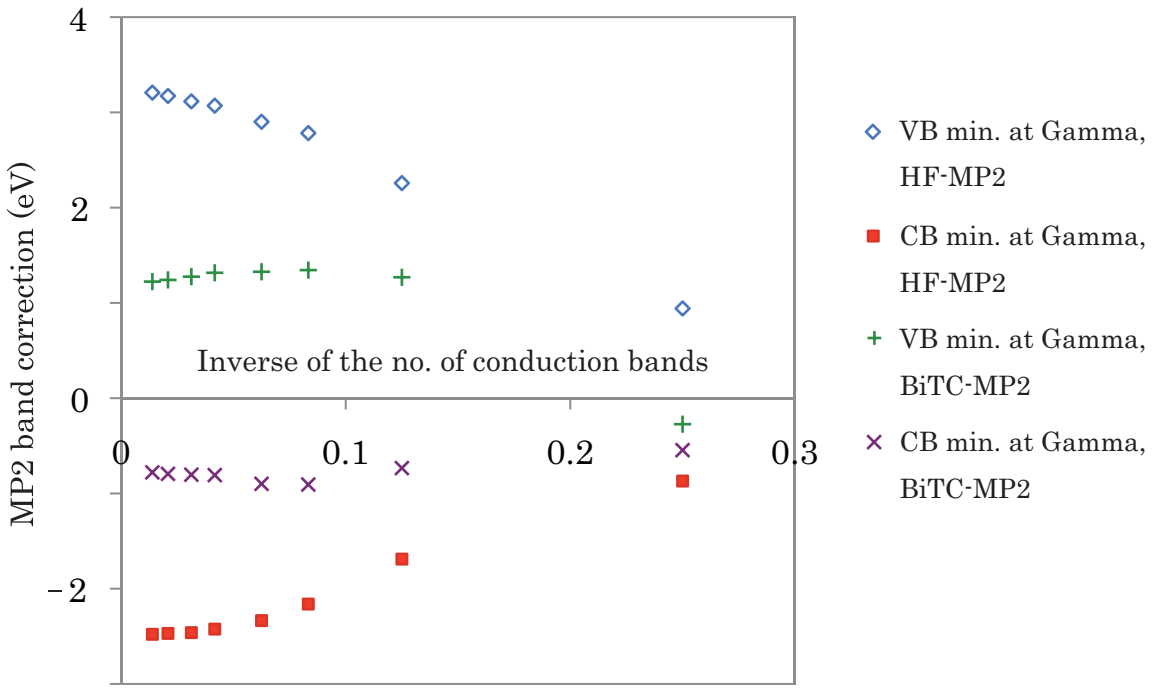

Figure 5.2: MP2 band corrections to the valence-band minimum and conduction-band minimum at the Γ point for silicon calculated using the HF-MP2 and BiTC-MP2 methods. These are relative values to the MP2 band corrections to the valence-band maximum at the Γ point, which are set to zero.

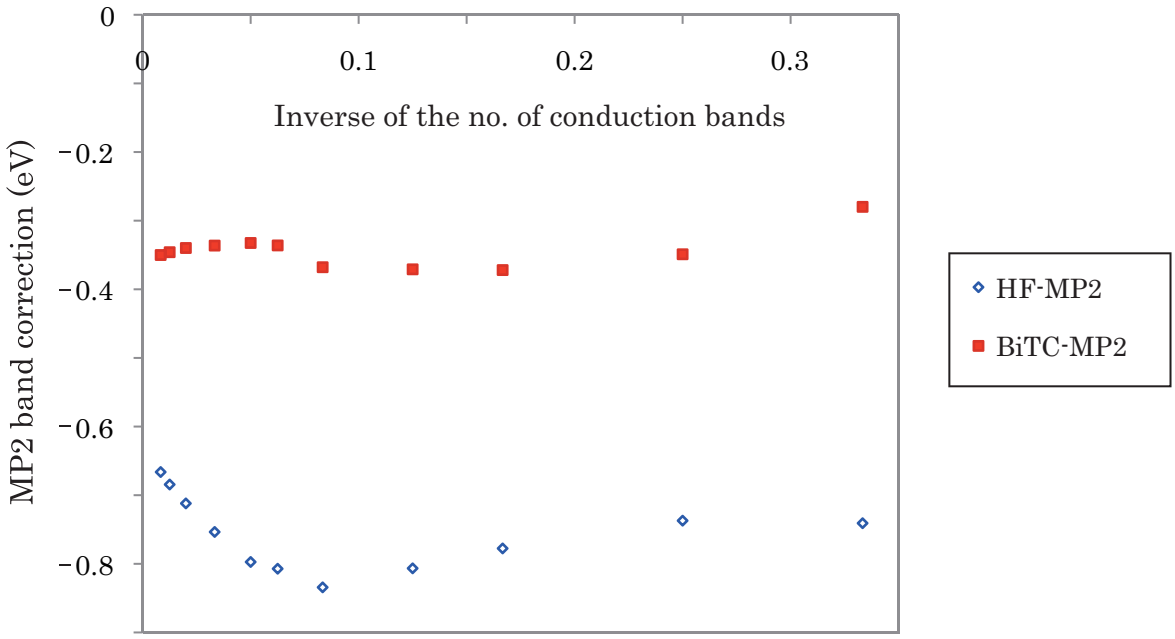

Figure 5.3: MP2 band corrections to the direct band gap for lithium hydride calculated using the HF-MP2 and BiTC-MP2 methods.

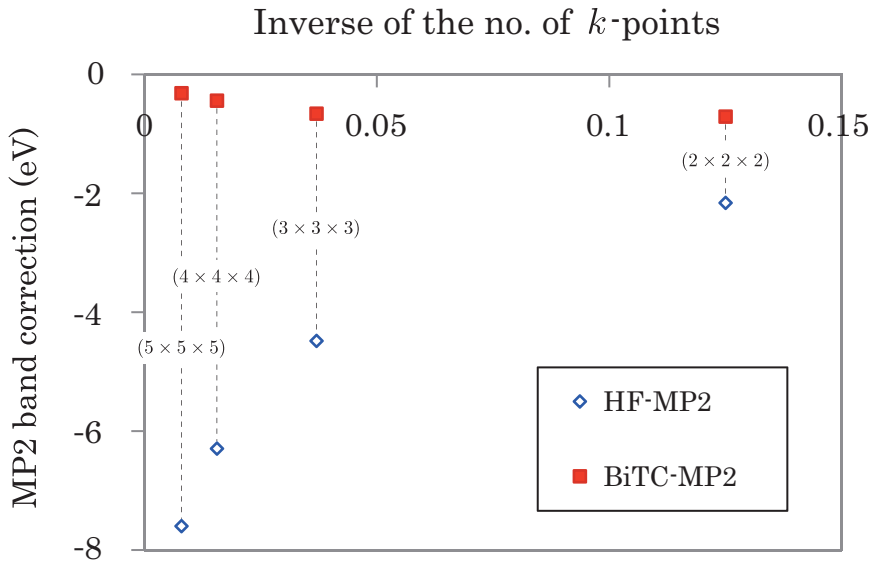

Figure 5.4: MP2 band corrections to the direct band gap at the Γ point for silicon calculated using the HF-MP2 and BiTC-MP2 methods.

	LDA	HF	HF-MP2	TC	BiTC	BiTC-MP2
R_{corr} (%)	90	0	102	109	110	89

Table 5.1: Valence correlation energy retrieved within our calculations R_{corr} (%), which is defined in Chapter 3, for each method.

5.6 Results: valence correlation energy

Valence correlation energy retrieved by our calculation, R_{corr} (%), which is defined in Chapter 3, for each method is listed in Table 5.1. MP2 correlation energies in this table were obtained by quadratic fitting with respect to the inverse of the number of k-points using results of $2\times2\times2$, $3\times3\times3$, and $4\times4\times4$ k-point meshes. For MP2 calculations, 16 Ry cutoff energy for plane waves, 100 LDA orbitals to expand one-electron orbitals of the HF and BiTC methods, and 4 (full) valence bands for excited configurations were used. Extrapolation with respect to the number of conduction bands for excited configurations was also performed. Since the reference DMC calculation and our calculations use a different pseudopotential, these values of the valence correlation energy should be considered only as a rough estimate of accuracy of these methods, but we can see all of these methods (except the HF method) give a good estimate of the total energy.

5.7 Results: band gaps

Band gaps of some simple solids calculated using the HF-MP2, BiTC-MP2, and several other methods are presented in Table 5.2. Ref. [51] uses the PAW method [101], somewhat different treatment of core electrons from the pseudopotential method we adopt here, but their results of the HF method are similar to ours. Differences between the HF-MP2 results of theirs and ours seem to be because (i) treatment of core electrons is different as mentioned above, (ii) they calculated the MP2 band correction with partially self-consistent manner, i.e., ϵ_v and ϵ_c are updated as $\epsilon_v^{\mathrm{HF-MP2}}$ and $\epsilon_c^{\mathrm{HF-MP2}}$, respectively, in an iterative manner in Eqs. (5.11) and (5.12), and/or (iii) convergence with the number of k-points is verified within a different amount of the error. Anyway, the calculated HF-MP2 band gaps show the same behavior; the MP2 corrections are too large for solids with relatively narrow band gaps, while for the wide-gap systems, the HF-MP2 method provides good accuracy. This tendency is natural because the MP2 perturbation theory cannot work for metallic systems, where the MP2 correlation energy diverges [102], and so can provide inaccurate results also for narrow-gap systems. As for the BiTC-MP2 method, the MP2 correction is very small except for lithium fluoride, where the band gap is improved. This situation seems to be because the BiTC method already retrieves a

	LDA	HF	HF (Ref. [51])	HF-MP2	HF-MP2 (Ref. [51])	TC	BiTC	BiTC-MP2	Exp.
Si (direct)	2.6	9.2	-	-0.1	-	4.6	4.6	4.4	3.40, 3.05[a]
Si (indirect)	0.5	6.7	7.1	-	-1.2	2.0	2.2	-	1.17[b]
SiC	1.4	8.9	8.7	-2.3	-0.8	3.2	3.9	4.0	2.4[c]
LiH	2.6	10.5	-	5.3	-	6.4	6.4	6.4	5.0[d]
LiF	9.9	21.7	21.8	14.6	14.2	14.0	17.1	14.8	14.2[e]

Table 5.2: Band gaps (eV) of some solids calculated with several methods. [a] From the compilation given in Ref. [92], [b] Ref. [40], [c] Ref. [41], [d] Ref. [42], [e] Ref. [44].

large part of the correlation energy without the MP2 perturbation. These results are a bit discouraging considering its expensive computational cost, and suggest that one should take other measures to take account of electron correlation effects not retrieved here and obtain the accurate band structures. To get some physical insights from these results, in the next section, we investigate the MP2 correction for the BiTC method in detail.

5.8 Role of the effective interaction in the TC Hamiltonian

We investigate a role of the effective interaction in the TC Hamiltonian for the MP2 correlation for further understanding of our results and the nature of the electron correlation effects that can be retrieved with our treatment.

Table 5.3 presents the MP2 correlation for the total energy per primitive cell of bulk silicon calculated with each condition: (i) HF-MP2, (ii) BiTC-MP2 with $v_{2\mathrm{body}}(x_1, x_2) = 1/|\mathbf{r}_1 - \mathbf{r}_2|$ and $v_{3\mathrm{body}}(x_1, x_2, x_3) = 0$ (i.e., only Coulomb interaction) in Eq. (5.8), (iii) BiTC-MP2 with

$$v_{2\mathrm{body}}(x_1, x_2) = \frac{1}{|\mathbf{r}_1 - \mathbf{r}_2|} + \frac{1}{2}(\nabla_1^2 u(x_1, x_2) + \nabla_2^2 u(x_1, x_2)) \tag{5.16}$$

$$= \frac{1}{|\mathbf{r}_1 - \mathbf{r}_2|}(1 - \alpha \exp[-\frac{|\mathbf{r}_1 - \mathbf{r}_2|}{C}]), \tag{5.17}$$

where $\alpha = 1/2$ (spin parallel), 1 (spin anti-parallel) and $v_{3\mathrm{body}}(x_1, x_2, x_3) = 0$ (i.e., partially canceled Coulomb interaction) in Eq. (5.8), (iv) BiTC-MP2 with full two-body interaction and $v_{3\mathrm{body}}(x_1, x_2, x_3) = 0$ (i.e., without three-body terms) in Eq. (5.8), and (v) BiTC-MP2 with full interaction both for two- and three-body terms. Note that, for (ii), (iii), and (iv), the BiTC-SCF equation was solved with full interaction, and only MP2 correction Eq. (5.7) was calculated with partial interaction. In the conditions (iii), (iv), and (v), divergence of the electron-electron Coulomb repulsion at $|\mathbf{r}_1 - \mathbf{r}_2| = 0$ is (partially) canceled with the effective two-body potential as seen in Eq. (5.17), which is considered to be an important contribution of the effective potential in the TC Hamiltonian for short-range correlation. We used a $2 \times 2 \times 2$ k-point mesh, 16 Ry cutoff energy for the plane

	(i) HF-MP2	(ii) BiTC-MP2 (partial)	(iii) BiTC-MP2 (partial)	(iv) BiTC-MP2 (partial)	(v) BiTC-MP2
MP2 correlation	-0.232	-0.320	-0.090	-0.043	-0.031

Table 5.3: MP2 correlation for the total energy per primitive cell (Hartree) calculated with each condition: (i) HF-MP2, (ii) only Coulomb interaction is used for calculating the BiTC-MP2 correction, (iii) partially canceled Coulomb interaction is used for calculating the BiTC-MP2 correction, (iv) BiTC-MP2 without three-body interaction, and (v) normal BiTC-MP2. Each condition is explained in detail in the main text.

wave, 100 LDA orbitals to expand one-electron orbitals in the HF and BiTC methods, and 4 (full) valence bands for excited configurations. Linearly extrapolated values of the MP2 correlation energies with respect to the inverse of the number of conduction bands N_{bc} using the MP2 correlation energies of $N_{bc} = 24$ and 32 were adopted.

First, comparing (i) with (ii), a difference between these two energies comes from differences of the one-electron orbitals and their orbital energies between the HF and BiTC methods. We verified that two kinds of orbitals are very similar, but the orbital energies exhibit a large difference as mentioned before: e.g., the band gap calculated with the HF method (about 7eV) is much larger than that for the BiTC method (about 2eV). This issue enlarges the MP2 correlation energy of the case (ii) (cf. Eq. (5.7)). Next, a difference among (ii), (iii), (iv), (v) suggests that the BiTC-MP2 correlation energy is largely affected by the effective two-body potential $\nabla^2 u$ rather than the other two-body and three-body potential in the TC Hamiltonian. The cancelation shown in Eq. (5.17) is due to the cusp condition imposed on the Jastrow factor, and so we can conclude that the cusp condition, which describes the short-range correlation, plays very important role for evaluation of the total energy of the BiTC-MP2 method.

On the other hand, as for the band structures, also the three-body terms have significant contribution. Table 5.4 presents the MP2 corrections to the band structures of bulk silicon calculated with the above-mentioned conditions of interactions, from (i) to (v), using a $4 \times 4 \times 4$ k-point mesh, 25 Ry cutoff energy for the plane wave, 100 LDA orbitals to expand one-electron orbitals in the HF and BiTC methods, and 4 (full) valence and 12 conduction bands for excited configurations. $\Gamma_{25'}$ and X_{1c} denote the maximum of the valence band at the Γ point and the minimum of the conduction bands at the X point, respectively. Note that the conduction-band minimum in the whole Brillouin zone lies in a middle way between the Γ and X points, but the MP2 band correction to this point is difficult to obtain, and so we calculated the transition energy between $\Gamma_{25'}$ and X_{1c} instead. We can see that not only the two-body potential in the TC Hamiltonian but also the three-body potential have a large contribution to the band energies comparing

	(i) HF-MP2	(ii) BiTC-MP2 (partial)	(iii) BiTC-MP2 (partial)	(iv) BiTC-MP2 (partial)	(v) BiTC-MP2
MP2 Correction to the valence-band width	-5.4	-12.8	-6.5	-10.3	-4.5
MP2 Correction to the direct gap at the Γ point	-6.3	-9.2	-6.7	-7.2	-0.4
MP2 Correction to the ($\Gamma_{25'}$ to X_{1c}) transition	-6.1	-8.6	-6.4	-6.4	0.0

Table 5.4: MP2 correction to the band structures (eV) for silicon calculated with each condition, which is explained in detail in the main text.

with the small contribution of the three-body potential to the total energy presented in Table 5.3. Three-body potential in the TC Hamiltonian describes the screening effect of the electron-electron Coulomb interaction in the long-range region as shown in Chapter 3.

We also performed the same calculations for the MP2 correction to the band gap of lithium fluoride. Table 5.5 presents the MP2 corrections calculated with the above-mentioned variations of interactions taken into account ((i) to (v)) using a $3 \times 3 \times 3$ k-point mesh, 81 Ry cutoff energy for the plane wave, 200 LDA orbitals to expand one-electron orbitals in the HF and BiTC methods, and 4 (full) valence and 20 conduction bands for excited configurations. We can see the same tendency as mentioned before; not only the two-body but also the three-body potential makes an important contribution to the MP2 correction to the band gap. Also, in Table 5.4 and 5.5, we can see that the other two-body potentials than $\nabla^2 u$ also have a large contribution, but the total contribution of the effective two-body potential yielded from the Jastrow function (i.e., a difference between (ii) and (iv)) is much smaller than those of the three-body potential (i.e., a difference between (iv) and (v)). At least for these materials, it is suggested that, to obtain the correct band structure, the effect of the three-body potential is essential and this is consistent with our study presented in Chapter 3; the long-range behavior of the Jastrow function is crucial for band structure calculations and will affect the screening effect described with the three-body potential. The knowledge obtained in Chapter 3 and here suggests that it is important for accurate band structure calculations to describe the screening effect in more rigorous manner comparing with the present treatment, where the screening is described with only one Jastrow parameter, 'A'. For this purpose, more general Jastrow functions such as $\sum_p w_p(\mathbf{r}) u_p(\mathbf{r}-\mathbf{r}') w_p(\mathbf{r}')$, or the CC theory, where infinite series of diagrams including the ring diagrams are considered [103], seem to be effective. A study in this direction is an important future issue.

	(i) HF-MP2	(ii) BiTC-MP2 (partial)	(iii) BiTC-MP2 (partial)	(iv) BiTC-MP2 (partial)	(v) BiTC-MP2
MP2 correlation	-5.9	-6.8	-3.0	-5.7	-2.7

Table 5.5: MP2 correlation to the band gap (eV) for lithium fluoride calculated with each condition, which is explained in detail in the main text.

Chapter 6

Configuration Interaction Singles (CIS) method

In the former chapters, we concentrate our attention on improvement of accuracy of the ground-state calculation. Another expected development for the TC method is to perform the excited-state calculation. In this chapter, we propose a new method for excited-state calculation using the TC Hamiltonian. In particular, we shall show that accurate optical absorption spectra of solids can be obtained by our method.

6.1 HF-CIS method

We briefly review the conventional configuration interaction singles (CIS) method based on the HF method [15]. In the HF method, the many-body wave function of the ground state is assumed to be the single Slater determinant: $\Phi_0 = (1/\sqrt{N!})\det[\phi_{1,\dots,N}(x_{1,\dots,N})]$. For the excited-state calculation, the simplest way is to use the CIS approximation, in which we assume the excited-state wave function to be the linear combination of the singly-excited configurations,

$$\Phi_i^a = (1/\sqrt{N!})\det[\phi_{1,\dots,\hat{i},\dots,N,a}(x_{1,\dots,N})], \tag{6.1}$$

where an electron of the i-th occupied state is excited to the a-th unoccupied state. In other words, the excited-state wave function Φ_{excited} is represented as

$$\Phi_{\text{excited}} = \sum_{i,a} c_{i,a}\Phi_i^a. \tag{6.2}$$

Then, the eigenvalue problem, $\mathcal{H}\Phi_{\text{excited}} = E_{\text{excited}}\Phi_{\text{excited}}$, can be solved as the following way: (i) solve an SCF equation in the HF method to obtain the optimized one-electron orbitals and their orbital energies, (ii) calculate the matrix elements $\langle\Phi_i^a|\mathcal{H}|\Phi_j^b\rangle$ (called the CI matrix), and (iii) diagonalize the CI matrix. By the diagonalization, one can obtain the coefficients $c_{i,a}$ in the Eq. (6.2), and the total energies E_{excited} for several excited states.

The CIS approximation is often used as the simplest way for the excited-state calculation because of its simple formalism and relatively low computational cost comparing with other wave function theories. It is noteworthy that one can deal with the excitonic effect by this method because the electron-hole interaction is taken into account in the above matrix elements.

For solid-state calculation, however, the conventional CIS method based on the HF method (we call it the HF-CIS method hereafter) has not enough accuracy to describe the electronic structure of the excited states. The reason is the same as that of the failure of the HF method applied to the solid-state calculations, that is, the HF-CIS method cannot describe the screening effect, resulting in, e.g., too strong exciton binding energy. Moreover, when we calculate the optical absorption spectrum, the calculated spectrum is shifted to the high-energy region owing to the overestimation of the band gap by the HF method. These features were investigated in recent studies [104, 49], and also we shall see them in a later section. To overcome these shortcomings, we combine the TC method with the CIS approximation, that we call the TC-CIS method.

6.2 TC-CIS method

In the TC-CIS method, we also use the singly-excited configurations, Eq. (6.1), and represent the excited-state wave function Ψ_{excited} as

$$\Psi_{\text{excited}} = F\Phi_{\text{excited}}, \tag{6.3}$$

$$\text{where } \Phi_{\text{excited}} = c_0\Phi_0 + \sum_{i,a} c_{i,a}\Phi_i^a. \tag{6.4}$$

An obvious difference between Eq. (6.2) and Eq. (6.4) is the existence of the term, $c_0\Phi_0$. In the HF-CIS, $c_0 = 0$ holds because of Hermiticity of the Hamiltonian [15], which does not hold for our non-Hermitian TC Hamiltonian. In other words, for the TC Hamiltonian, $\langle\Phi_0|\mathcal{H}_{TC}|\Phi_i^a\rangle$ does not equal zero. (cf. Appendix A.) Electron correlation effect is partially taken into account through the similarity-transformation of the Hamiltonian with the Jastrow factor F, the same as the ground-state calculation.

TC-CIS calculation is performed in the same way as that of the HF-CIS method, though the CIS approximation (Eq. (6.4)) is now applied to the similarity-transformed Hamiltonian (TC Hamiltonian), $\mathcal{H}_{TC}$. In this thesis, we calculate the optical absorption spectrum of solids using the TC-CIS method. For this purpose, states i and a in Φ_i^a should have the same crystal momentum because the momentum transfer between light and condensed matter is negligibly small.

Some approximations for the TC-CIS method

We developed two techniques of the approximations used in the calculations of the optical absorption spectrum using the TC-CIS method, which is indispensable to have their computational cost practical.

The calculation of the CI-matrix elements appears to be computationally expensive because its cost scales as $\mathcal{O}(N_k^3)$ owing to the three-body terms in the TC Hamiltonian, where N_k is the number of k-points. However, many part of the three-body terms can be calculated at $\mathcal{O}(N_k^2)$ cost using a technique used in the ground-state calculation [25], e.g., the term,

$$\sum_q \langle ajq|\nabla_2 u(x_{21})\nabla_2 u(x_{23})|bqi\rangle, \tag{6.5}$$

where a and b denote the indices of the unoccupied states, and i, j, and q denote those of the occupied states, is calculated as follows:

$$\text{calculate (i) } f^1_{q,i}(x_3) \equiv \phi^*_q(x_3)\phi_i(x_3), \tag{6.6}$$

$$\text{(ii) } f^2_{q,i}(x_2) \equiv \int \mathrm{d}x_3 \nabla_2 u(x_{23}) f^1_{q,i}(x_3), \tag{6.7}$$

$$\text{(iii) } f^3_i(x_2) \equiv \sum_q \phi_q(x_2) f^2_{q,i}(x_2), \tag{6.8}$$

$$\text{(iv) } f^4_{i,j}(x_2) \equiv \phi^*_j(x_2) f^3_i(x_2), \tag{6.9}$$

$$\text{(v) } f^5_{i,j}(x_1) \equiv \int \mathrm{d}x_2 \nabla_2 u(x_{21}) f^4_{i,j}(x_2), \tag{6.10}$$

$$\text{(vi) } f^6_{i,j,a}(x_1) \equiv \phi^*_a(x_1) f^5_{i,j}(x_1), \tag{6.11}$$

$$\text{(vii) } \int \mathrm{d}x_1 f^6_{i,j,a}(x_1)\phi_b(x_1). \tag{6.12}$$

Because a and i (also b and j, respectively) have the same crystal momentum, i.e., Φ^a_i (and Φ^b_j) has the same total crystal momentum as Φ_0, the above-mentioned calculations require only $\mathcal{O}(N_k^2)$ computational cost. We verified that the remaining two kinds of terms that require $\mathcal{O}(N_k^3)$ computational cost,

$$\sum_q \langle ajq|\nabla_1 u(x_{12})\nabla_1 u(x_{13})|bqi\rangle, \text{ and} \tag{6.13}$$

$$\sum_q \langle ajq|\nabla_2 u(x_{21})\nabla_2 u(x_{23})|qib\rangle, \tag{6.14}$$

yield small contributions to the optical absorption spectra for the materials focused on in this work (LiF and GaAs). Figure 6.1 shows the calculated optical absorption spectra of solid LiF using a $4 \times 4 \times 4$ k-point mesh with and without an approximation, for which one does not calculate the above-mentioned expensive three-body terms Eq. (6.13) and (6.14) that require $\mathcal{O}(N_k^3)$ computational cost. We can see that the neglected terms affect

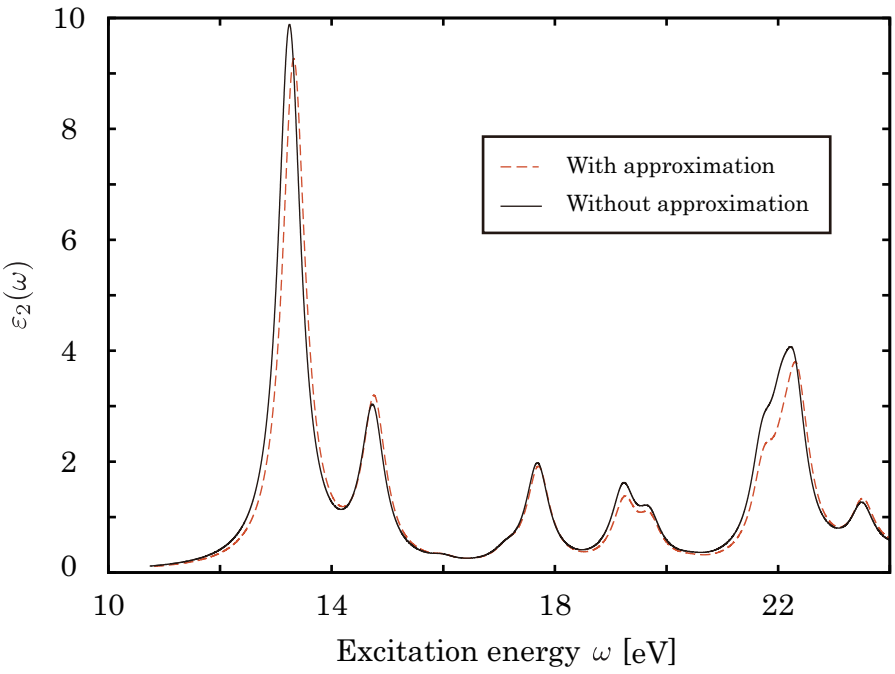

Figure 6.1: Calculated optical absorption spectra of LiF using a $4 \times 4 \times 4$ k-point mesh with (dashed line) and without (solid line) the approximation mentioned in the body text.

little to the calculated absorption spectrum of LiF, and the same also holds for GaAs, so we shall adopt this approximation.

We also face another difficulty in calculating the optical absorption spectrum. The optical absorption spectrum is obtained from the imaginary part of the dielectric function $\epsilon_2(\omega)$,

$$\epsilon_2(\omega) = (\frac{2\pi}{\omega})^2 \sum_n \frac{|\langle F\Phi_0|\mathbf{e}_\lambda \cdot \nabla|F\Phi_n\rangle|^2}{\langle F\Phi_0|F\Phi_0\rangle\langle F\Phi_n|F\Phi_n\rangle}\delta(\omega - (E_n - E_0)), \tag{6.15}$$

where n denotes an index of an excited state, and $\mathbf{e}_\lambda$ a polarization vector of the photon. However, evaluation of this quantity requires evaluation of a $3N$-dimensional integrations, which is computationally very demanding. To avoid doing this integration for this study, we calculate

$$(\frac{2\pi}{\omega})^2 \sum_n \frac{|\langle F^{-1}\Phi_0|\mathbf{e}_\lambda \cdot \nabla|F\Phi_n\rangle|^2}{\langle \Phi_0|\Phi_0\rangle\langle \Phi_n|\Phi_n\rangle}\delta(\omega - (E_n - E_0)), \tag{6.16}$$

instead of Eq. (6.15). The relation between these two quantities is described as follows: first,

$$\frac{|\langle F^{-1}\Phi_0|\mathbf{e}_\lambda \cdot \nabla|F\Phi_n\rangle|^2}{\langle \Phi_0|\Phi_0\rangle\langle \Phi_n|\Phi_n\rangle} = \frac{|\langle F^{-1}\Phi_0|(\sum_j \frac{|F\Phi_j\rangle\langle F\Phi_j|}{\langle F\Phi_j|F\Phi_j\rangle})\mathbf{e}_\lambda \cdot \nabla|F\Phi_n\rangle|^2}{\langle \Phi_0|\Phi_0\rangle\langle \Phi_n|\Phi_n\rangle}, \tag{6.17}$$

holds where j is summed over all eigenstates of $\mathcal{H}$. Next, we suppose $|\langle \Phi_0|\Phi_j\rangle| \ll \langle \Phi_0|\Phi_0\rangle$

for $j \neq 0$, and hence we only consider the $j = 0$ term in Eq. (6.17). This yields

$$\text{Eq. (6.17)} \simeq \frac{|\langle F\Phi_0|\mathbf{e}_\lambda \cdot \nabla|F\Phi_n\rangle|^2}{\langle F\Phi_0|F\Phi_0\rangle\langle F\Phi_n|F\Phi_n\rangle} \times \frac{\langle\Phi_0|\Phi_0\rangle\langle F\Phi_n|F\Phi_n\rangle}{\langle F\Phi_0|F\Phi_0\rangle\langle\Phi_n|\Phi_n\rangle}. \tag{6.18}$$

In addition, assuming $\langle F\Phi_0|F\Phi_0\rangle/\langle\Phi_0|\Phi_0\rangle \simeq \langle F\Phi_n|F\Phi_n\rangle/\langle\Phi_n|\Phi_n\rangle$, the latter factor in Eq. (6.18) becomes 1, and therefore we find that Eq. (6.15) and Eq. (6.16) are approximately the same. The approximations we used here are not easily validated, but we shall see that obtained spectra possess sufficient accuracy for a quantitative discussion. Eq. (6.16) involves $F^{-1}\nabla F = \nabla - \sum_{i<j}(\nabla_i + \nabla_j)u(\mathbf{r}_i, \mathbf{r}_j)$, which is easy to be evaluated, and in particular, when we use the Jastrow function satisfying $u(\mathbf{r}_i, \mathbf{r}_j) = u(\mathbf{r}_i - \mathbf{r}_j)$, $F^{-1}\nabla F = \nabla$ holds.

Computational cost

As we have seen, computational cost to evaluate the CI-matrix elements such as $\langle\Phi_i^a|\mathcal{H}_{TC}|\Phi_j^b\rangle$ is originally $\mathcal{O}(N_k^3)$ but can be reduced to $\mathcal{O}(N_k^2)$ by neglecting few expensive terms with slight change of the calculated spectrum. To mention in detail, the computational cost scales as $\mathcal{O}(N_k^2 N_{bv}^2 N_{bc}^2 N_{pw})$, where N_{bv}, N_{bc}, and N_{pw} are the numbers of the occupied, unoccupied bands, and plane waves to expand one-electron orbitals, respectively.

Actually, diagonalization of the CI matrix requires $\mathcal{O}(N_k^3 N_{bv}^3 N_{bc}^3)$ cost because the size of the matrix is determined by the number of singly excited configurations ($= \mathcal{O}(N_k N_{bv} N_{bc})$). Because this diagonalization does not involve $\mathcal{O}(N_{pw})$ or $\mathcal{O}(N_{pw}\log N_{pw})$ calculations, it depends on the conditions of calculations which is more expensive, the diagonalization or the calculation of the matrix elements.

6.3 Results: optical absorption spectra of solid LiF and GaAs

Conditions

All conditions described in Chapter 3 were used also in this chapter. Experimental lattice constants (7.59 Bohr for LiF [105] and 10.68 Bohr for GaAs [106]) were used. In this chapter, we used the Jastrow function optimized following a way mentioned in Chapter 3.2:

$$u(x, x') = \frac{A}{|\mathbf{r} - \mathbf{r}'|}\left(1 - \exp\left(-\frac{|\mathbf{r} - \mathbf{r}'|}{C_{\sigma,\sigma'}}\right)\right), \tag{6.19}$$

where $A = \sqrt{1 - (1/\varepsilon)} \times A_0 = \sqrt{1 - (1/\varepsilon)} \times \sqrt{V/(4\pi N)}$ (ε: the dielectric constant calculated with an RPA relation using LDA orbitals, N: the number of valence electrons, V: the volume) and $C_{\sigma,\sigma'} = \sqrt{2A}$ (spin parallel: $\sigma = \sigma'$), $\sqrt{A}$ (spin anti-parallel: $\sigma \neq \sigma'$).

Long-range behavior of this function was determined to reproduce the screened electron-electron interaction in solids as $1/r \to 1/(\varepsilon r)$, and short-range behavior was determined by imposing the cusp condition, as we have seen in previous chapter. Using this Jastrow function, these electron correlation effects are taken into consideration through the TC Hamiltonian. The values of A/A_0 were 0.7264 for LiF and 0.9596 for GaAs.

Optical absorption spectra of solid LiF

First, we calculated the optical absorption spectrum of solid LiF, which is known for its very strongly bound exciton. Figure 6.2 presents the optical absorption spectra calculated using the TC-CIS and HF-CIS methods with a $10 \times 10 \times 10$ k-point mesh, 81 Ry cutoff energy for plane waves, and 100 LDA orbitals for the expansion of the one-electron orbitals for both the HF and TC methods. Three valence bands and six conduction bands from the Fermi energy were used for electron excitation. We can see the overall structure of the experimental spectrum is well reproduced with both the TC-CIS and HF-CIS methods. However, the HF-CIS method has two problems. First, the band gap is heavily overestimated in the HF level, and therefore, the spectrum is shifted to the high-energy region. Second, the exciton binding energy for the HF-CIS method is over 4eV, which is much larger than the experimental value, from 1.4 to 1.9eV [44]. Recall that the binding energy is defined as the difference between the energy corresponding to the sharp excitonic peak (see Figure 6.2) and the direct band gap at the Γ point obtained with the ground-state calculation. This large derivation reflects the fact that the HF-CIS method cannot describe the screening effect of the electron-electron interaction, yielding overbinding exciton. The TC-CIS method notably overcomes these problems and yields a surprisingly accurate spectrum. The band gap is correctly reproduced and the exciton binding energy is about 1.5eV, which falls within the range of experimental values. Our simple Jastrow factor enables an accurate description of the electronic structure in solids, including the exciton.

Optical absorption spectra of solid GaAs

Next, we calculated the optical absorption spectra of solid GaAs, presented in Figure 6.3. We used a $10 \times 10 \times 10$ k-point mesh, 36 Ry cutoff energy for plane waves, 80 LDA orbitals in the expansion of the one-electron orbitals, and three valence bands and six conduction bands from the Fermi energy for electron excitation. For this material, we shifted the k-point mesh where electron excitations occur for $-0.01\mathbf{b}_1 - 0.02\mathbf{b}_2 + 0.03\mathbf{b}_3$ with $\{\mathbf{b}_1, \mathbf{b}_2, \mathbf{b}_3\}$ being the basic reciprocal-lattice vectors. The idea to use a shifted grid to achieve a good spectral resolution was originally proposed by Rohlfing and Louie [108], and using this constant shift is the same way as Ref. [109]. In using the HF-CIS method,

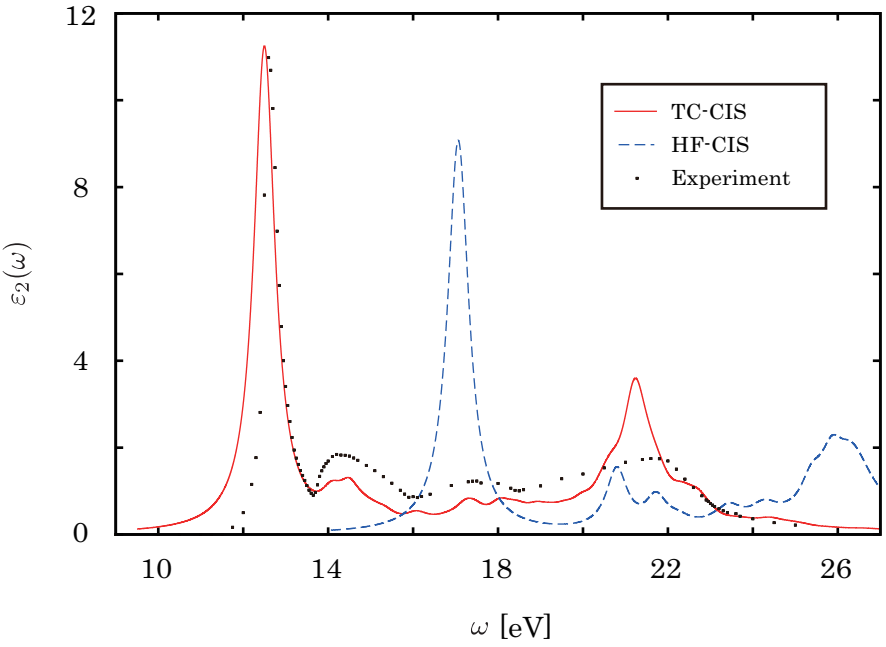

Figure 6.2: Calculated optical absorption spectra of LiF using the TC-CIS (solid line) and HF-CIS (dashed line) methods. Broadening is performed using the Lorentz function $f(x; x_0, \gamma) = (1/\pi)(\gamma/((x - x_0)^2 + \gamma^2))$ with $\gamma = 0.3$eV. Experimental data [107] are represented by dots.

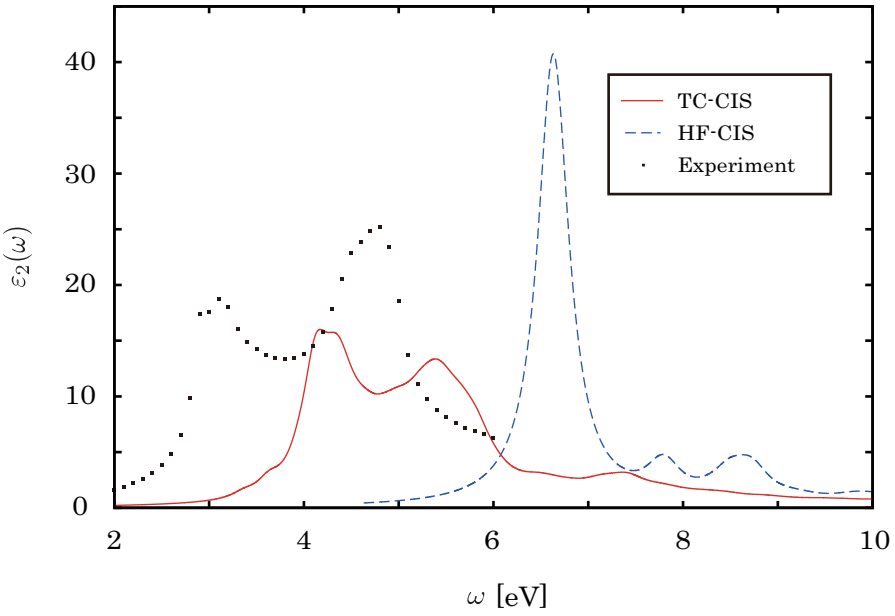

Figure 6.3: Calculated optical absorption spectra of GaAs using the TC-CIS (solid line) and HF-CIS (dashed line) methods. Broadening is performed using the Lorentz function with $\gamma = 0.15$ and 0.2eV for the TC-CIS and HF-CIS methods, respectively. Experimental data [111] are represented by dots.

there is a large discrepancy between the experimental data and the calculated spectrum, where we see a large shift of the whole spectrum to the high-energy region and a wrong strongly-bound excitonic peak with very strong intensity. The direct band gap calculated using the HF method is 7.8 eV, and hence the calculated exciton binding energy is about 1eV, whereas experimentally it is a few meV with very small intensity [110]. These trends in the results from the HF-CIS method are similar to those of LiF. Although the spectrum calculated with the TC-CIS method is also shifted to the high-energy region, through the overestimation of the band gap in the ground-state calculation, the characteristic two peaks are reproduced.

Discussion

The TC-CIS method well reproduces the experimental spectra, both for the sharp excitonic peak of LiF and for the entire structure of both LiF and GaAs. To obtain a more accurate spectrum of small-gap systems like GaAs, an accurate prediction of the band gap for small-gap systems in the TC calculation is indispensable. For this purpose, the correlation effects not captured with our simple treatment will be necessary by means of, e.g., combination of the TC method with more elaborate post-HF methods described in the former chapters.

While we use the TC method (not the BiTC method) in this chapter, the BiTC-CIS

method can be performed in a similar, but slightly different manner. In the BiTC-CIS method, $c_0 = 0$ holds in Eq. (6.4) because the Brillouin's theorem holds (see, Appendix A). However, the major difference is the difference between the calculated band gaps with the TC method and those with the BiTC method, which largely affects the accuracy of the obtained optical absorption spectrum.

Although similar or sometimes better agreement with experiment can be obtained by using GW+BSE [54, 55, 56] or time-dependent DFT with long-range kernels [112, 113, 114], an accurate description of the spectra based on the first-principles wave function theory, i.e., using a many-body wave function explicitly, is helpful to understand how we describe electron correlations by means of such wave functions, and will be the basis for systematic improvements in the spectral calculations. The success of our rather simple formalism suggests great potential of the wave function theory for excited-state calculations of solids. In addition, we believe that some approximation techniques we developed in this work are valuable also for other wave-function-based theories when obtaining the optical absorption spectra.

Interestingly, although our TC-CIS method is an apparently different approach from the GW+BSE method, which is well known as an accurate method based on the many-body perturbation theory for excited-state calculation, there are some interesting similarities. The screening effect of the electron-electron interaction is described by the Jastrow factor in the TC method, and by the screened interaction W in GW; also, the CIS approximation is usually used also in GW+BSE calculations as the Tamm-Dancoff approximation. Some examples of the differences between the two methods are: (i) the screening effect is described by only one parameter in our Jastrow factor, which is too simple compared with the way screening is considered in GW+BSE, and (ii) the cusp condition is taken into account by the Jastrow factor in the TC-CIS method whereas it is difficult to do so in GW+BSE. Such differences can lead to the differences observed in the calculated spectra. (cf., Ref. [56].) In the TC-CIS method, it is advantageous that one can obtain the total energy of the excited state, which can be utilized to find the stable structure of the excited state in future application.

Chapter 7

Conclusion

In this thesis, we achieved theoretical improvements for the TC method by two ways and apply them to the band structure calculations and excited state calculations of solids.

First, in Chapter 3, we developed a new method to optimize the Jastrow factor with reasonable computational cost and applied this method to some simple solids. We found that the long-range behavior of the Jastrow function largely affects the band structures of solids while the short-range polynomial terms does not so much. The former results relate to the strength of the screening effect of the electron-electron interaction, which corresponds to the 'A' parameter in the Jastrow function and is determined using the value of the dielectric constant. The latter results suggest that our simple Jastrow function that is a function of $|\mathbf{r} - \mathbf{r}'|$ does not have enough accuracy. In terms of the computational cost, the long-range parameter is determined very efficiently by our RPA treatment. Also pseudo-variance minimization to optimize short-range parameters requires reasonable computational cost, but this cost was found to be comparable to usual QMC calculations. Despite this fact, development of our new formalism has two significances. First, we obtain another efficient way to optimize the Jastrow factor in addition to QMC. This is helpful to check validity of optimization ansatz and compare accuracy of calculations with each other. Moreover, because pseudo-variance minimization does not employ the local energy or local variance as used in QMC, one can easily apply our method also to somewhat ill-conditioned Jastrow functions, e.g., those not satisfying the cusp condition. This means that our method exhibits robustness in some situations and it can be helpful for some kinds of theoretical investigation.

Next, in Chapter 5, the MP2 perturbation theory combined with the BiTC method was applied to solid-state calculations. We found that the BiTC-MP2 method shows favorable convergence behavior because a large part of the correlation energy is already retrieved at the BiTC level and so the MP2 correction for the BiTC method is much smaller than that for the HF method. However, because of such a small amount of the

correction, MP2 treatment changes the band gaps of the BiTC method very little except for lithium fluoride, and so satisfactory improvement of accuracy is not achieved for most solids calculated in this thesis. Observation presented in this chapter suggests that, to obtain the accurate band structures, we should describe the screening effect in more rigorous manner than the present treatment, in which the screening effect is described with the only one Jastrow parameter, 'A'. Description of the screening effect can be improved by using more sophisticated Jastrow functions such as $\sum_p w_p(\mathbf{r})u_p(\mathbf{r}-\mathbf{r}')w_p(\mathbf{r}')$ or those with more complex long-range behavior, or by combining with more sophisticated wave function theories such as the CC theory, which takes account of infinite series of diagrams including the ring diagrams. These treatments will also improve the description of the short-range correlation effects.

As a result of the improvement in accuracy, in Chapter 6, the excited-state calculations were performed using the TC-CIS method with the optimized Jastrow factor. We showed that the accurate optical absorption spectra are obtained with our rather simple formalism using the optimized Jastrow factor and the linear combination of the singly excited configurations. This is an important step for future development of the excited-state calculations based on the wave function theory. Moreover, it is meaningful to verify that our simple wave function is able to describe the screened electron-hole interaction and the formation of the exciton by this interaction in an intuitive manner.

For applying the first-principles calculations to broad types of materials including the strongly correlated systems, improvement of the accuracy is a very important and urgent problem. A comprehensive study of the TC method for solid-state calculations presented in this thesis provided a new insight about how we can take account of the electron correlation effects by using the explicitly correlated wave functions. We believe that our strategy to make use of the Jastrow-Slater-type many-body wave function is verified to be powerful, efficient, intuitive, and promising for high-accuracy calculation; the Jastrow factor retrieves a large part of the electron correlation and the Slater determinant allows one to employ the band picture. Important future issues are to use the more general Jastrow factor, which is suggested by our study of Jastrow optimization (Chapter 3) and MP2 (Chapter 5), and to combine the TC method with sophisticated wave function theories such as the CC theory. These studies require massive computational effort, but will provide important insight to understand the nature of the electron correlation effects.

It is also desirable to use the TC method for exploring the stable structures of solids because availability of the Hellmann-Feynman force is an important advantage of the (Bi)TC method, and in several cases a slight energy difference is crucial for predicting the stable structure; high-accuracy calculation is required. This is an important future problem, which may require to develop the pseudopotential for the TC method, and to investigate the Hellmann-Feynman force in the TC method in detail.

Appendix A

Brillouin's theorem for the TC method

We provide a proof of the Brillouin's theorem for the TC method here, which states that

$$\langle \Phi_i^a | \mathcal{H}_{\mathrm{TC}} | \Phi_0 \rangle = 0, \tag{A.1}$$

for any singly excited configuration Φ_i^a defined as $\Phi_i^a \equiv (1/\sqrt{N!})\det[\phi_{1,2,\ldots,\hat{i},\ldots,N-1,N,a}(x_{1,\ldots,N})]$, where an electron of the i-th occupied state is excited to the a-th unoccupied state. This relation is easily verified by explicitly calculating the left-hand side of Eq. (A.1) as follows:

$$\begin{aligned}
&\text{LHS of Eq. (A.1)} \\
&= \int \mathrm{d}x_1 \ \phi_a^*(x_1)\Big(-\frac{1}{2}\nabla_1^2 + v_{\mathrm{ext}}(x_1)\Big)\phi_i(x_1) \\
&\quad + \sum_{j=1}^{N} \int \mathrm{d}x_1 \mathrm{d}x_2 \ \phi_a^*(x_1)\phi_j^*(x_2) v_{\mathrm{2body}}(x_1, x_2) \det[\phi_{i,j}(x_{1,2})] \\
&\quad - \frac{1}{2}\sum_{j=1}^{N}\sum_{k=1}^{N} \int \mathrm{d}x_1 \mathrm{d}x_2 \mathrm{d}x_3 \ \phi_a^*(x_1)\phi_j^*(x_2)\phi_k^*(x_3) \\
&\qquad\qquad \times v_{\mathrm{3body}}(x_1, x_2, x_3) \det[\phi_{i,j,k}(x_{1,2,3})] \\
&= \int \mathrm{d}x_1 \ \phi_a^*(x_1) \sum_{j=1}^{N} \epsilon_{ij}\phi_j(x_1) \quad (\because \text{Eq. (2.10)}) \\
&= 0 \quad (\because \phi_a \text{ is orthogonal to every } \phi_i.)
\end{aligned} \tag{A.2}$$

Note that $\langle \Phi_0 | \mathcal{H}_{\mathrm{TC}} | \Phi_i^a \rangle \neq 0$ is caused by the non-Hermiticity of the TC Hamiltonian. However, if we use a biorthogonal formulation of the TC method, we can obtain the Brillouin's theorem for both sides: $\langle X_0 | \mathcal{H}_{\mathrm{TC}} | \Phi_i^a \rangle = \langle X_i^a | \mathcal{H}_{\mathrm{TC}} | \Phi_0 \rangle = 0$ where X is the left determinant appearing in the biorthogonal formulation [95]. Contents in this appendix is

published under licence in *J. Phys.: Conf. Ser.* by IOP Publishing Ltd. (M. Ochi and S. Tsuneyuki, *J. Phys.: Conf. Ser.* **454** 012020 (2013). http://iopscience.iop.org/1742-6596/454/1/012020).

Acknowledgment

First and foremost, I would like to express my deepest gratitude to my supervisor, Prof. Shinji Tsuneyuki, for his insightful suggestions and sincere encouragement for this work. Without his great guidance at crucial points, this dissertation would not have been possible. Also, his continuing support has enabled me to attend many conferences and have great experience with many researchers. I am grateful to Dr. Yoshihiro Gohda for his incisive comments and valuable advices on this work. Computational resources he provided me were indispensable for this study. Also, his comments on the study of physics sometimes in the university or sometimes outside (over a bottle) are invaluable for my research life. Dr. Keitaro Sodeyama has given useful advices and warm encouragement from the beginning of my research. My study employs the TC++ code, which was originally developed by Dr. Rei Sakuma. I have received persistent help from secretaries, Ms. Makiko Fukuda, Ms. Chiharu Yoshioka, Ms. Kaori Sugiura, Ms. Yuko Yoshida, and Ms. Keiko Onoda for many clerical works on my research activities. I also appreciate wide-ranging discussion and constant encouragement by all the members in Tsuneyuki Research Group. I was much stimulated by their interesting studies and cheered by their kind personalities. In particular, Mr. Yoshiyuki Yamamoto gave helpful advices and constructive discussion with him is invaluable. In this group, I had wonderful experiences as a researcher under blessed environment. This work was supported by a Grant-in-Aid for JSPS Fellows and the Computational Materials Science Initiative. Computations were performed at the supercomputer center of the Institute for Solid State Physics, The University of Tokyo, and the K computer at the RIKEN Advanced Institute for Computational Science (proposal number hp120086). Finally, I would like to express cordial gratitude to my family members, Shigeyuki, Mariko, Eriko, and Nadesiko (a cat).

Bibliography

[1] P. Hohenberg and W. Kohn. *Phys. Rev.*, 136:B864, 1964.

[2] W. Kohn and L. J. Sham. *Phys. Rev.*, 140:A1133, 1965.

[3] J. F. Janak. *Phys. Rev. B*, 18:7165, 1978.

[4] J. P. Perdew and A. Zunger. *Phys. Rev. B*, 23:5048, 1981.

[5] J. P. Perdew, K. Burke, and M. Ernzerhof. *Phys. Rev. Lett.*, 77:3865, 1996.

[6] J. P. Perdew, K. Burke, and M. Ernzerhof. *Phys. Rev. Lett.*, 78:1396, 1997.

[7] A. D. Becke. *J. Chem. Phys.*, 98:5648, 1993.

[8] C. Adamo and V. Barone. *J. Chem. Phys.*, 110:6158, 1999.

[9] J. Heyd, G. E. Scuseria, and M. Ernzerhof. *J. Chem. Phys.*, 118:8207, 2003.

[10] T. Koopmans. *Physica*, 1:104, 1934.

[11] R. Dovesi, C. Pisani, and C. Roetti. *Int. J. Quantum Chem.*, 17:517, 1980.

[12] R. Dovesi, C. Pisani, F. Ricca, and C. Roetti. *Phys. Rev. B*, 22:5936, 1980.

[13] R. Dovesi, C. Pisani, C. Roetti, and P. Dellarole. *Phys. Rev. B*, 24:4170, 1981.

[14] N. W. Ashcroft and N. D. Mermin. *Solid State Physics.* Holt, Rinehart and Winston, 1976.

[15] A. Szabo and N. S. Ostlund. *Modern Quantum Chemistry: Introduction to Advanced Electronic Structure Theory.* Macmillan, New York, 1982.

[16] S. F. Boys and N. C. Handy. *Proc. R. Soc. London Ser. A*, 309:209, 1969.

[17] S. F. Boys and N. C. Handy. *Proc. R. Soc. London Ser. A*, 310:43, 1969.

[18] S. F. Boys and N. C. Handy. *Proc. R. Soc. London Ser. A*, 310:63, 1969.

[19] S. F. Boys and N. C. Handy. *Proc. R. Soc. London Ser. A*, 311:309, 1969.

[20] N. C. Handy. *Mol. Phys.*, 21:817, 1971.

[21] S. Ten-no. *Chem. Phys. Lett.*, 330:169, 2000.

[22] S. Ten-no. *Chem. Phys. Lett.*, 330:175, 2000.

[23] N. Umezawa and S. Tsuneyuki. *J. Chem. Phys.*, 119:10015, 2003.

[24] R. Sakuma and S. Tsuneyuki. *J. Phys. Soc. Jpn.*, 75:103705, 2006.

[25] M. Ochi, K. Sodeyama, R. Sakuma, and S. Tsuneyuki. *J. Chem. Phys.*, 136:094108, 2012.

[26] H. Luo, W. Hackbusch, and H.-J. Flad. *Mol. Phys.*, 108:425, 2010.

[27] H. Luo. *J. Chem. Phys.*, 133:154109, 2010.

[28] G. I. Kerley. *Phys. Rev. B*, 10:1255, 1974. The role of the Jastrow function was investigated and a similar result was obtained with a different choice of the Jastrow function.

[29] N. Umezawa and S. Tsuneyuki. *Phys. Rev. B*, 69:165102, 2004.

[30] T. Kato. *Commun. Pure Appl. Math.*, 10:151, 1957.

[31] W. M. C. Foulkes, L. Mitas, R. J. Needs, and G. Rajagopal. *Rev. Mod. Phys.*, 73:33, 2001.

[32] J. Kolorenč, S. Hu, and L. Mitas. *Phys. Rev. B*, 82:115108, 2010.

[33] R. Prasad, N. Umezawa, D. Domin, R. Salomon-Ferrer, and W. A. Lester, Jr. *J. Chem. Phys.*, 126:164109, 2007.

[34] L. Mitáš and R. M. Martin. *Phys. Rev. Lett.*, 72:2438, 1994.

[35] A. J. Williamson, Randolph Q. Hood, R. J. Needs, and G. Rajagopal. *Phys. Rev. B*, 57:12140, 1998.

[36] N. Umezawa and S. Tsuneyuki. *J. Chem. Phys.*, 121:7070, 2004.

[37] Y. Suzuki and H. Matsumura. *Prog. Theor. Phys.*, 113:87, 2005.

[38] S. Tsuneyuki. *Prog. Theor. Phys. Supplement*, 176:134, 2008.

[39] S. Ten-no. *Chem. Phys. Lett.*, 353:317, 2002.

[40] C.Kittel. *Introduction to Solid State Physics, 6th ed.* Wiley, New York, 1986.

[41] P. Y. Yu and M. Cardona. *Fundamentals of Semiconductors, 3rd corrected ed.* Springer-Verlag, Berlin, 2005.

[42] V. G. Plekhanov, A. A. O'Connell-Bronin, and T. A. Betenekova. *Fiz. Tverd. Tela*, 19:3297, 1977.

[43] G. Baldini and B. Bosacchi. *Phys. Status Solidi*, 38:325, 1970.

[44] M. Piacentini, D. W. Lynch, and C. G. Olson. *Phys. Rev. B*, 13:5530, 1976.

[45] L. Hedin. *Phys. Rev.*, 139:A796, 1965.

[46] M. S. Hybertsen and S. G. Louie. *Phys. Rev. Lett.*, 55:1418, 1985.

[47] M. S. Hybertsen and S. G. Louie. *Phys. Rev. B*, 34:5390, 1986.

[48] V. Polo, E. Kraka, and D. Cremer. *Mol. Phys.*, 100:1771, 2002.

[49] M. Lorenz, L. Maschio, M. Schütz, and D. Usvyat. *J. Chem. Phys.*, 137:204119, 2012.

[50] I. Gadaczek, K. J. Hintze, and T. Bredow. *Phys. Chem. Chem. Phys.*, 14:741, 2012.

[51] A. Grüneis, M. Marsman, and G. Kresse. *J. Chem. Phys.*, 133:074107, 2010.

[52] M. Marsman, A. Grüneis, J. Paier, and G. Kresse. *J. Chem. Phys.*, 130:184103, 2009.

[53] G. H. Booth, A. Grüneis, G. Kresse, and A. Alavi. *Nature*, 493:365, 2013.

[54] S. Albrecht, L. Reining, R. Del Sole, and G. Onida. *Phys. Rev. Lett.*, 80:4510, 1998.

[55] L. X. Benedict, E. L. Shirley, and R. B. Bohn. *Phys. Rev. Lett.*, 80:4514, 1998.

[56] M. Rohlfing and S. G. Louie. *Phys. Rev. Lett.*, 81:2312, 1998.

[57] I. Duchemin and F. Gygi. *Comput. Phys. Commun.*, 181:855, 2010.

[58] S. Fantoni and S. Rosati. *Nuovo Cimento A*, 25:593, 1975.

[59] E. Krotscheck and M. L. Ristig. *Nucl. Phys. A*, 242:389, 1975.

[60] J. G. Zabolitzky. *Phys. Rev. A*, 16:1258, 1977.

[61] E. Manousakis, S. Fantoni, V. R. Pandharipande, and Q. N. Usmani. *Phys. Rev. B*, 28:3770, 1983.

[62] E. Krotscheck, W. Kohn, and G.-X. Qian. *Phys. Rev. B*, 32:5693, 1985.

[63] M. D. Towler, Randolph Q. Hood, and R. J. Needs. *Phys. Rev. B*, 62:2330, 2000.

[64] L. Mitas and R. M. Martin. *Phys. Rev. Lett.*, 72:2438, 1994.

[65] J. Kolorenč and L. Mitas. *Phys. Rev. Lett.*, 101:185502, 2008.

[66] J. Kolorenč and L. Mitas. *Rev. Mineral. Geochem.*, 71:137, 2010.

[67] L. Mitas. *Comput. Phys. Commun.*, 96:107, 1996.

[68] S. A. Khairallah and B. Militzer. *Phys. Rev. Lett.*, 101:106407, 2008.

[69] G. Rajagopal, R. J. Needs, A. James, S. D. Kenny, and W. M. C. Foulkes. *Phys. Rev. B*, 51:10591, 1995.

[70] M. W. C. Dharma-wardana and F. Grimaldi. *Phys. Rev. A*, 13:1702, 1976.

[71] E. A. G. Amour. *J. Phys. C: Solid St. Phys.*, 13:343, 1980.

[72] D. Ceperley. *Phys. Rev. B*, 18:3126, 1978.

[73] D. Bohm and D. Pines. *Phys. Rev.*, 92:609, 1953.

[74] F. Gygi and A. Baldereschi. *Phys. Rev. B*, 34:4405, 1986.

[75] N. D. Drummond, M. D. Towler, and R. J. Needs. *Phys. Rev. B*, 70:235119, 2004.

[76] R. Gaudoin, M. Nekovee, W. M. C. Foulkes, R. J. Needs, and G. Rajagopal. *Phys. Rev. B*, 63:115115, 2001.

[77] M. Gajdoš, K. Hummer, G. Kresse, J. Furthmüller, and F. Bechstedt. *Phys. Rev. B*, 73:045112, 2006.

[78] C. J. Umrigar, K. G. Wilson, and J. W. Wilkins. *Phys. Rev. Lett.*, 60:1719, 1988.

[79] T. Shimazaki and So Hirata. *Int. J. Quant. Chem.*, 13:2953, 2009.

[80] N. D. Drummond and R. J. Needs. *Phys. Rev. B*, 72:085124, 2005.

[81] C. G. Broyden. *J. Inst. Math. Appl.*, 6:222, 1970.

[82] R. Fletcher. *Computer J.*, 13:317, 1970.

[83] D. Goldfarb. *Math. Comp.*, 24:23, 1970.

[84] D. F. Shanno. *Math. Comp.*, 24:647, 1970.

[85] N. Troullier and J. L. Martins. *Phys. Rev. B*, 43:1993, 1991.

[86] S. Massidda, M. Posternak, and A. Baldereschi. *Phys. Rev. B*, 48:5058, 1993.

[87] J. Yamauchi, M. Tsukada, S. Watanabe, and O. Sugino. *Phys. Rev. B*, 54:5586, 1996.

[88] O. Sugino and A. Oshiyama. *Phys. Rev. Lett.*, 68:1858, 1992.

[89] E. Staritzky and D. I. Walker. *Anal. Chem.*, 28:1055, 1956.

[90] M. J. L. Sangster, U. Schröder, and R. M. Atwood. *J. Phys. C*, 11:1523, 1978.

[91] H. V. Nguyen and S. Gironcoli. *Phys. Rev. B*, 79:205114, 2009.

[92] M. Rohlfing, P. Krüger, and J. Pollmann. *Phys. Rev. B*, 48:17791, 1993.

[93] K. Ichikawa, N. Suzuki, and K. Tsutsumi. *J. Phys. Soc. Jpn.*, 50:3650, 1981.

[94] W. J. Choyke and L. Patrick. *Phys. Rev.*, 187:1041, 1969.

[95] O. Hino, Y. Tanimura, and S. Ten-no. *J. Chem. Phys.*, 115:7865, 2001.

[96] H. Hellmann. *Einführung in die Quantenchemie*. Leipzig: Franz Deuticke, 1937.

[97] R. P. Feynman. *Phys. Rev.*, 56:340, 1939.

[98] L. Schimka, J. Harl, and G. Kresse. *J. Chem. Phys.*, 134:024116, 2011.

[99] S. Suhai. *Phys. Rev. B*, 27:3506, 1983.

[100] J. J. Shepherd, A. Grüneis, G. H. Booth, G. Kresse, and A. Alavi. *Phys. Rev. B*, 86:035111, 2012.

[101] P. E. Blöchl. *Phys. Rev. B*, 50:17953, 1994.

[102] M. Gell-Mann and K. A. Brueckner. *Phys. Rev.*, 106:364, 1957.

[103] G. E. Scuseria, T. M. Henderson, and D. C. Sorensen. *J. Chem. Phys.*, 129:231101, 2008.

[104] M. Lorenz, D. Usvyat, and M. Schütz. *J. Chem. Phys.*, 134:094101, 2011.

[105] C. A. Hutchison and H. L. Johnston. *J. Am. Chem. Soc.*, 62:3165, 1940.

[106] R. C. Weast. *Handbook of Chemistry and Physics 61st ed.* CRC, Boca Raton, 1980.

[107] D. M. Roessler and W. C. Walker. *J. Opt. Soc. Am.*, 57:835, 1967.

[108] M. Rohlfing and S. G. Louie. *Phys. Rev. B*, 62:4927, 2000.

[109] K. Nakamura, Y. Yoshimoto, R. Arita, S. Tsuneyuki, and M. Imada. *Phys. Rev. B*, 77:195126, 2008.

[110] D. D. Sell. *Phys. Rev. B*, 6:3750, 1972.

[111] D. E. Aspnes and A. A. Studna. *Phys. Rev. B*, 27:985, 1983.

[112] L. Reining, V. Olevano, A. Rubio, and G. Onida. *Phys. Rev. Lett.*, 88:066404, 2002.

[113] P. L. de Boeij, F. Kootstra, J. A. Berger, R. van Leeuwen, and J. G. Snijders. *J. Chem. Phys.*, 115:1995, 2001.

[114] Y.-H. Kim and A. Görling. *Phys. Rev. Lett.*, 89:096402, 2002.